

# Physics potential of the CERN–MEMPHYS neutrino oscillation project

J.-E. Campagne<sup>a</sup>, M. Maltoni<sup>b</sup>, M. Mezzetto<sup>c</sup>, and T. Schwetz<sup>d</sup>

<sup>a</sup>*Laboratoire de l'Accélérateur Linéaire, IN2P3-CNRS and University PARIS-SUD 11  
Centre Scientifique d'Orsay-Bât. 200-B.P. 34, 91898 Orsay Cedex, France*

<sup>b</sup>*International Centre for Theoretical Physics, Strada Costiera 11, 31014 Trieste, Italy*

<sup>c</sup>*Istituto Nazionale Fisica Nucleare, Sezione di Padova, Via Marzolo 8, 35100 Padova, Italy*

<sup>d</sup>*Scuola Internazionale Superiore di Studi Avanzati, Via Beirut 2–4, 34014 Trieste, Italy*

## Abstract

We consider the physics potential of CERN based neutrino oscillation experiments consisting of a Beta Beam ( $\beta$ B) and a Super Beam (SPL) sending neutrinos to MEMPHYS, a 440 kt water Čerenkov detector at Fréjus, at a distance of 130 km from CERN. The  $\theta_{13}$  discovery reach and the sensitivity to CP violation are investigated, including a detailed discussion of parameter degeneracies and systematical errors. For  $\beta$ B and SPL sensitivities similar to the ones of the phase II of the T2K experiment (T2HK) are obtained, where the results for the CERN–MEMPHYS experiments are less affected by systematical uncertainties. We point out that by a combination of data from  $\beta$ B and SPL a measurement with antineutrinos is not necessary and hence the same physics results can be obtained within about half of the measurement time compared to one single experiment. Furthermore, it is shown how including data from atmospheric neutrinos in the MEMPHYS detector allows to resolve parameter degeneracies and, in particular, provides sensitivity to the neutrino mass hierarchy and the octant of  $\theta_{23}$ .

# 1 Introduction

In recent years strong evidence for neutrino oscillations has been obtained in solar [1], atmospheric [2], reactor [3], and accelerator [4] neutrino experiments. The very near future of long-baseline (LBL) neutrino experiments is devoted to the study of the oscillation mechanism in the range of  $\Delta m_{31}^2 \approx 2.4 \times 10^{-3} \text{ eV}^2$  indicated by atmospheric neutrinos using conventional  $\nu_\mu$  beams. Similar as in the K2K experiment in Japan [4], the presently running MINOS experiment in the USA [5] uses a low energy beam to measure  $\Delta m_{31}^2$  by observing the  $\nu_\mu \rightarrow \nu_\mu$  disappearance probability, while the forthcoming OPERA [6] experiment will be able to detect  $\nu_\tau$  appearance within the high energy CERN–Gran Sasso beam [7]. If we do not consider the LSND anomaly [8] that will be further studied soon by the MiniBooNE experiment [9], all data can be accommodated within the three flavor scenario (see Refs. [10,11] for recent global analyses), and neutrino oscillations are described by two neutrino mass-squared differences ( $\Delta m_{21}^2$  and  $\Delta m_{31}^2$ ) and the  $3 \times 3$  unitary Pontecorvo-Maki-Nakagawa-Sakata (PMNS) lepton mixing matrix [12] with three angles ( $\theta_{12}, \theta_{13}, \theta_{23}$ ) and one Dirac CP phase  $\delta_{\text{CP}}$ .

Future tasks of neutrino physics are an improved sensitivity to the last unknown mixing angle,  $\theta_{13}$ , to explore the CP violation mechanism in the leptonic sector, and to determine the sign of  $\Delta m_{31}^2$  which describes the type of the neutrino mass hierarchy (normal,  $\Delta m_{31}^2 > 0$  or inverted,  $\Delta m_{31}^2 < 0$ ). The present upper bound on  $\theta_{13}$  is dominated by the constraint from the Chooz reactor experiment [13]. A global analysis of all data yields  $\sin^2 2\theta_{13} < 0.082$  at 90% CL [11]. A main purpose of upcoming reactor and accelerator experiments is to improve this bound or to reveal a finite value of  $\theta_{13}$ . In reactor experiments, one uses  $\bar{\nu}_e$  in disappearance mode and the sensitivity is increased with respect to present experiments by the use of a near detector close to the reactor [14]. In accelerator experiments, the first generation of so-called Super Beams with sub-mega watt proton drivers such as T2K (phase-I) [15] and NO $\nu$ A [16], the appearance channel  $\nu_\mu \rightarrow \nu_e$  is explored. This next generation of reactor and Super Beam experiments will reach sensitivities of the order of  $\sin^2 2\theta_{13} \lesssim 0.01$  (90% CL) within a time scale of several years [17]. Beyond this medium term program, there are several projects on how to enter the high precision age in neutrino oscillations and to attack the ultimate goals like the discovery of leptonic CP violation or the determination of the neutrino mass hierarchy. In accelerator experiments, one can extend the Super Beam concept by moving to multi-mega watt proton drivers [15,18–20] or apply novel technologies, such as neutrino beams from decaying ions (so-called Beta Beams) [21,22] or from decaying muons (so-called Neutrino Factories) [22,23].

In this work we focus on possible future neutrino oscillation facilities hosted at CERN, namely a multi-mega watt Super Beam experiment based on a Super Proton Linac (SPL) [24] and a  $\gamma = 100$  Beta Beam ( $\beta\text{B}$ ) [25]. These experiments will search for  $\bar{\nu}_\mu \rightarrow \bar{\nu}_e$  and  $\bar{\nu}_e \rightarrow \bar{\nu}_\mu$  appearance, respectively, by sending the neutrinos to a mega ton scale water Čerenkov detector (MEMPHYS) [26], located at a distance of 130 km from CERN under the Fréjus mountain. Similar detectors are under consideration also in the US (UNO [27]) and in Japan (Hyper-K [15,28]). We perform a detailed analysis of the SPL and  $\beta\text{B}$  physics potential, discussing the discovery reach for  $\theta_{13}$  and leptonic CP violation. In addition we consider the possibility to resolve parameter degeneracies in the LBL data by using the atmospheric neutrinos available in the mega ton detector [29]. This leads to a sensitivity to the neutrino mass hierarchy of the CERN–MEMPHYS experiments, despite the rather short baseline.

	$\beta$ B	SPL	T2HK
Detector mass	440 kt	440 kt	440 kt
Baseline	130 km	130 km	295 km
Running time ( $\nu + \bar{\nu}$ )	5 + 5 yr	2 + 8 yr	2 + 8 yr
Beam intensity	$5.8 (2.2) \cdot 10^{18}$ He (Ne) dcys/yr	4 MW	4 MW
Systematics on signal	2%	2%	2%
Systematics on backgr.	2%	2%	2%

**Table 1:** Summary of default parameters used for the simulation of the  $\beta$ B, SPL, and T2HK experiments.

The physics performances of  $\beta$ B and SPL are compared to the ones obtainable at the second phase of the T2K experiment in Japan, which is based on an upgraded version of the original T2K beam and the Hyper-K detector (T2HK) [15].

The outline of the paper is as follows. In Sec. 2 we summarize the main characteristics of the  $\beta$ B, SPL, and T2HK experiments and give general details of the physics analysis methods, whereas in Sec. 3 we describe in some detail the MEMPHYS detector, the  $\beta$ B, and the SPL Super Beam. In Sec. 4 we review the problem of parameter degeneracies and discuss its implications for the experiments under consideration. In Sec. 5 we present the sensitivities to the “atmospheric parameters”  $\theta_{23}$  and  $\Delta m_{31}^2$ , the  $\theta_{13}$  discovery potential, and the sensitivity to CP violation. We also investigate in some detail the impact of systematical errors. In Sec. 6 we discuss synergies which are offered by the CERN–MEMPHYS facilities. We point out advantages of the case when  $\beta$ B and SPL are available simultaneously, and we consider the use of atmospheric neutrino data in MEMPHYS in combination with the LBL experiments. Our results are summarized in Sec. 7.

## 2 Experiments overview and analysis methods

In this section we give the most important experimental parameters which we adopt for the simulation of the CERN–MEMPHYS experiments  $\beta$ B and SPL, as well as for the T2HK experiment in Japan. These parameters are summarized in Tab. 1. For all experiments the detector mass is 440 kt, and the running time is 10 years, with a division in neutrino and antineutrino running time in such a way that roughly an equal number of events is obtained. We always use the total available information from appearance as well as disappearance channels including the energy spectrum. For all three experiments we adopt rather optimistic values for the systematical uncertainties of 2% as default values, but we also consider the case when systematics are increased to 5%. These errors are uncorrelated between the various signal channels (neutrinos and antineutrinos), and between signals and backgrounds.

A more detailed description of the CERN–MEMPHYS experiments is given in Sec. 3. For the T2HK simulation we use the setup provided by GLoBES [30] based on Ref. [31], which follows closely the LOI [15]. In order to allow a fair comparison we introduce the following changes with respect to the configuration used in Ref. [31]: The fiducial mass is set to 440 kt, the systematical errors on the background and on the  $\nu_e$  and  $\bar{\nu}_e$  appearance signals is set to 2%, and we use a total running time of 10 years, divided into 2 years of data taking with neutrinos and 8 years with antineutrinos. Furthermore, we use the same CC

	$\beta\text{B}$		$\text{SPL}$		$\text{T2HK}$	
	$\delta_{\text{CP}} = 0$	$\delta_{\text{CP}} = \pi/2$	$\delta_{\text{CP}} = 0$	$\delta_{\text{CP}} = \pi/2$	$\delta_{\text{CP}} = 0$	$\delta_{\text{CP}} = \pi/2$
appearance $\nu$						
background	113		600		1017	
$\sin^2 2\theta_{13} = 0$	24		41		84	
$\sin^2 2\theta_{13} = 10^{-3}$	66	76	93	10	181	18
$\sin^2 2\theta_{13} = 10^{-2}$	285	314	387	126	754	240
appearance $\bar{\nu}$						
background	127		500		1428	
$\sin^2 2\theta_{13} = 0$	23		36		90	
$\sin^2 2\theta_{13} = 10^{-3}$	64	10	74	104	188	261
$\sin^2 2\theta_{13} = 10^{-2}$	271	100	297	390	746	977
disapp. $\nu$						
background	98178		21033		25038	
background	5		1		118	
disapp. $\bar{\nu}$						
background	72762		15731		34793	
background	6		1		148	

**Table 2:** Number of events for appearance and disappearance signals and backgrounds for the  $\beta\text{B}$ ,  $\text{SPL}$ , and  $\text{T2HK}$  experiments as defined in Tab. 1. For the appearance signals the event numbers are given for several values of  $\sin^2 2\theta_{13}$  and  $\delta_{\text{CP}} = 0$  and  $\pi/2$ . The background as well as the disappearance event numbers correspond to  $\theta_{13} = 0$ . For the other oscillation parameters the values of Eq. (1) are used.

detection cross section as for the  $\beta\text{B}/\text{SPL}$  analysis [32]. For more details see Refs. [15, 31].

In Tab. 2 we give the number of signal and background events for the experiment setups as defined in Tab. 1. For the appearance channels ( $\nu_{e \rightarrow \mu}^{(-)}$  for the  $\beta\text{B}$  and  $\nu_{\mu \rightarrow e}^{(-)}$  for  $\text{SPL}$  and  $\text{T2HK}$ ) we give the signal events for various values of  $\theta_{13}$  and  $\delta_{\text{CP}}$ . The “signal” events for  $\theta_{13} = 0$  are appearance events induced by the oscillations with  $\Delta m_{21}^2$ . The value  $\sin^2 2\theta_{13} = 10^{-3}$  corresponds roughly to the sensitivity limit for the considered experiments, whereas  $\sin^2 2\theta_{13} = 10^{-2}$  gives a good sensitivity to CP violation. This can be appreciated by comparing the values of  $\nu$  and  $\bar{\nu}$  appearance events for  $\delta_{\text{CP}} = 0$  and  $\pi/2$ . In the table the background to the appearance signal is given for  $\theta_{13} = 0$ . Note that in general the number of background events depends also on the oscillation parameters, since also the background neutrinos in the beam oscillate. This effect is consistently taken into account in the analysis, however, for the parameter values in the table the change in the background events due to oscillations is only of the order of a few events.

The physics analysis is performed with the  $\text{GLOBES}$  open source software [30], which provides a convenient tool to simulate long-baseline experiments and compare different facilities in a unified framework. The experiment definition (AEDL) files for the  $\beta\text{B}$  and  $\text{SPL}$  simulation with  $\text{GLOBES}$  are available at Ref. [33]. In the analysis parameter degeneracies and correlations are fully taken into account and in general all oscillation parameters are varied in the fit. To simulate the “data” we adopt the following set of “true values” for the

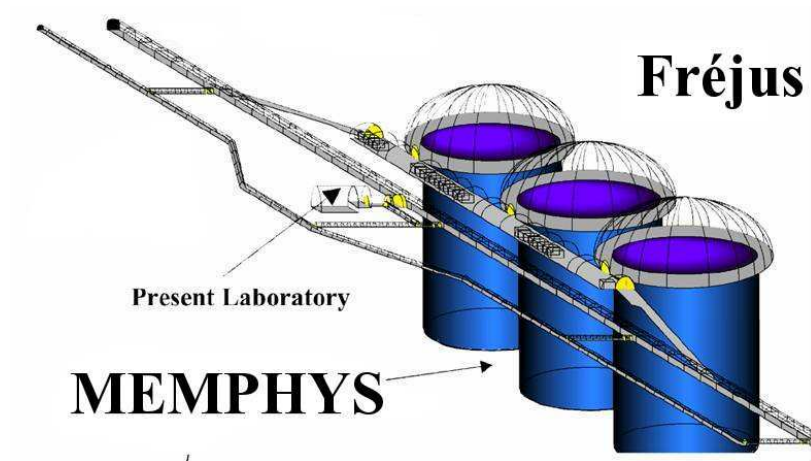


**Figure 1:** Sketch of the MEMPHYS detector under the Fréjus mountain.

oscillation parameters:

$$\begin{aligned} \Delta m_{31}^2 &= +2.4 \times 10^{-3} \text{ eV}^2, & \sin^2 \theta_{23} &= 0.5, \\ \Delta m_{21}^2 &= 7.9 \times 10^{-5} \text{ eV}^2, & \sin^2 \theta_{12} &= 0.3, \end{aligned} \quad (1)$$

and we include a prior knowledge of these values with an accuracy of 10% for  $\theta_{12}$ ,  $\theta_{23}$ ,  $\Delta m_{31}^2$ , and 4% for  $\Delta m_{21}^2$  at  $1\sigma$ . These values and accuracies are motivated by recent global fits to neutrino oscillation data [10, 11], and they are always used except where explicitly stated otherwise.

### 3 The CERN–MEMPHYS experiments

#### 3.1 The MEMPHYS detector

MEMPHYS (MEgaton Mass PHYSisics) [26] is a mega ton class water Čerenkov detector in the straight extrapolation of Super-Kamiokande, located at Fréjus, at a distance of 130 km from CERN. It is an alternative design of the UNO [27] and Hyper-Kamiokande [28] detectors and shares the same physics case, both from the non-accelerator domain (nucleon decay, super nova neutrino detection, solar neutrinos, atmospheric neutrinos) and from the accelerator domain which is the subject of this paper. A recent civil engineering pre-study to envisage the possibly of large cavity excavation located under the Fréjus mountain (4800 m.e.w.) near the present Modane underground laboratory has been undertaken. The main result of this pre-study is that MEMPHYS may be built with present techniques as a modular detector consisting of several shafts, each with 65 m in diameter, 65 m in height for the total water containment. A schematic view of the layout is shown in Fig. 1. For the present study we have chosen a fiducial mass of 440 kt which means 3 shafts and an inner detector (ID) of 57 m in diameter and 57 m in height. Each ID may be equipped with photo detectors (PMT, HPD, *etc.*) with a surface coverage of at least 30%. In principle up to 5 shafts are possible, corresponding to a fiducial mass of 730 kt. The Fréjus site offers a natural protection against cosmic rays by a factor  $10^6$ . If not mentioned otherwise, the event selection and particle identification are the Super-Kamiokande algorithms results.

	$^{18}\text{Ne}$			$^6\text{He}$		
	$\nu_\mu$ CC	$\pi^+$	$\pi^-$	$\bar{\nu}_\mu$ CC	$\pi^+$	$\pi^-$
Generated ev.	139181	863	561	107571	952	819
Particle ID	105923	209	123	83419	242	170
Decay	67888	103	6	67727	117	7

**Table 3:** Events for the  $\beta\text{B}$  in a 4400 kt yr exposure.  $\nu_\mu$  ( $\bar{\nu}_\mu$ ) CC events are computed assuming full oscillations ( $P_{\nu_e \rightarrow \nu_\mu} = 1$ ), and pion backgrounds are computed from  $\nu_e$  ( $\bar{\nu}_e$ ) CC+NC events. In the rows we give the number events generated within the fiducial volume (“Generated ev.”), after muon particle identification (“Particle ID”), and after applying a further identification requiring the detection of the Michel electron (“Decay”).

### 3.2 The $\gamma = 100 \times 100$ baseline Beta Beam

The concept of a Beta Beam ( $\beta\text{B}$ ) has been introduced by P. Zucchelli in Ref. [21]. Neutrinos are produced by the decay of radioactive isotopes which are stored in a decay ring. An important parameter is the relativistic gamma factor of the ions, which determines the energy of the emitted neutrinos.  $\beta\text{B}$  performances have been computed previously for  $\gamma(^6\text{He}) = 66$  [25], 100 [34–36], 150 [36], 200 [37], 350 [36], 500 [37, 38], 1000 [37], 2000 [38], 2488 [39]. A review can be found in Ref. [40], the physics potential of a very low gamma  $\beta\text{B}$  has been studied in Ref. [41]. Performances of a  $\beta\text{B}$  with  $\gamma > 150$  are extremely promising but rather speculative, because they are neither based on an existing accelerator complex nor on a robust estimation of the ion decay rates. For a CERN based  $\beta\text{B}$ , fluxes have been estimated in Ref. [42]. The infrastructure available at CERN as well as the the MEMPHYS location at a distance of 130 km suggest a  $\gamma$ -factor of about 100. Such a value implies a mean neutrino energy of 400 MeV, which leads to the oscillation maximum at about 200 km for  $\Delta m_{31}^2 = 2.4 \times 10^{-3} \text{ eV}^2$ . We have checked that the performance at the somewhat shorter baseline of 130 km is rather similar to the one at the oscillation maximum. Moreover, the purpose of this paper is to estimate the physics potential for a realistic set-up and not to study the optimization of the  $\beta\text{B}$  regardless of any logistic consideration (see, e.g., Refs. [36, 37] for such optimization studies).

The signal events from the  $\nu_e \rightarrow \nu_\mu$  neutrino and antineutrino appearance channels in the  $\beta\text{B}$  are  $\nu_\mu$  charged current (CC) events. The selection for these events is based on standard Super-Kamiokande particle identification algorithms. The muon identification is reinforced by asking for the detection of the Michel decay electron. Charged pions generated in NC events (or in NC-like events where the leading muon goes undetected) are the main source of background for the experiment. To compute this background inclusive NC and CC events have been generated with the  $\beta\text{B}$  spectrum. Events have been selected where the only visible track is a charged pion above the Čerenkov threshold. Particle identification efficiencies have been applied to those particles. The probability for a pion to survive in water until its decay has been computed with Geant 3.21 and cross-checked with a Fluka 2003 simulation. This probability is different for positive and negative pions, the latter having a higher probability to be absorbed before decaying. The surviving events are background, and the reconstructed neutrino energy is computed misidentifying these pions as muons. Event rates are reported in Tab. 3. From these numbers it becomes evident that requiring the detection of the Michel

electron provides an efficient cut to eliminate the pion background. These background rates are significantly smaller than quoted in Ref. [34], where pion decays were computed with the same probabilities as for muons. The numbers of Tab. 3 have been cross-checked by comparing the Nuance [43] and Neugen [44] event generators and in case of differences we have adopted the more pessimistic result.

Also atmospheric neutrinos can constitute an important source of background [21]. This background can be suppressed only by keeping a very short duty cycle, and this in turn is one of the most challenging bounds on the design of the Beta Beam complex. Following Ref. [45] we include the atmospheric neutrino background based on a Monte Carlo simulation using Nuance [43]. See also Ref. [45] for a discussion of the effect of a higher duty cycle. As pointed out in Ref. [36], it is necessary to use a migration matrix for the neutrino energy reconstruction to properly handle the Fermi motion smearing in the  $\gamma = 100 \beta\text{B}$  energy range. The matrices, computed with Nuance, have 25 true energy bins and 5 reconstructed energy bins in the range  $0 < E_\nu < 1 \text{ GeV}$ , see Ref. [45]. As shown in that reference the migration matrix approximation has a visible (though small) effect for example in the leptonic CP violation discovery potential.

### 3.3 The 3.5-GeV SPL Super Beam

In the Conceptual Design Report 1 (CDR1) the foreseen Super Proton Linac (SPL) [19] has been optimized to provide the protons for the muon production in the context of a Neutrino Factory. Recently, in Ref. [24] a new optimization of the beam energy as well as the secondary particle focusing and decay has been undertaken considering a Super Beam searching for  $\nu_\mu \rightarrow \nu_e$  and  $\bar{\nu}_\mu \rightarrow \bar{\nu}_e$  appearance as well as  $\nu_\mu, \bar{\nu}_\mu$  disappearance in a mega ton scale water Čerenkov detector. In particular, a full simulation of the beam line from the proton on target interaction up to the secondary particle decay tunnel has been performed. The proton on a liquid mercury target (30 cm long, 7.5 mm radius, 13.546 density) has been simulated with FLUKA 2002.4 [46] while the horn focusing system and the decay tunnel simulation has been performed with GEANT 3.21 [47].<sup>1</sup>

Since the optimization requirements for a Neutrino Factory are rather different than for a Super Beam the new SPL configuration has a significant impact on the physics performance (see Ref. [24] for a detailed discussion). The SPL fluxes of the four neutrino species ( $\nu_\mu, \nu_e, \bar{\nu}_\mu, \bar{\nu}_e$ ) for the positive ( $\nu_\mu$  beam) and the negative focusing ( $\bar{\nu}_\mu$  beam) are show in Fig. 2. The total number of  $\nu_\mu$  ( $\bar{\nu}_\mu$ ) in positive (negative) focusing is about  $1.18$  ( $0.97$ )  $\times 10^{12} \text{ m}^{-2} \text{ y}^{-1}$  with an average energy of 300 MeV. The  $\nu_e$  ( $\bar{\nu}_e$ ) contamination in the  $\nu_\mu$  ( $\bar{\nu}_\mu$ ) beam is around 0.7% (6.0%). Following Ref. [49], the  $\pi^0$  background is reduced using a tighter PID cut compared to standard Super-Kamiokande analysis. The Michel electron is required for the  $\mu$  identification. For the  $\nu_\mu \rightarrow \nu_e$  channel the background consists roughly of 90%  $\nu_e \rightarrow \nu_e$  CC interactions, 6%  $\pi^0$  from NC interactions, 3% miss identified muons from  $\nu_\mu \rightarrow \nu_\mu$  CC, and 1%  $\bar{\nu}_e \rightarrow \bar{\nu}_e$  CC interactions. For the  $\bar{\nu}_\mu \rightarrow \bar{\nu}_e$  channel the contributions to the background are 45%  $\bar{\nu}_e \rightarrow \bar{\nu}_e$  CC interactions, 35%  $\nu_e \rightarrow \nu_e$  CC interactions, 18%  $\pi^0$  from NC interactions

---

<sup>1</sup>Although there are differences between the predicted pion and kaon productions as a function of proton kinetic energy with FLUKA 2002.4 and 2005.6, the results are consistent for the relevant energy of 3.5 GeV. We emphasize that the pion and the kaon production cross-sections are waiting for experimental confirmation [48] and a new optimization would be required if their is a disagreement with the present knowledge.

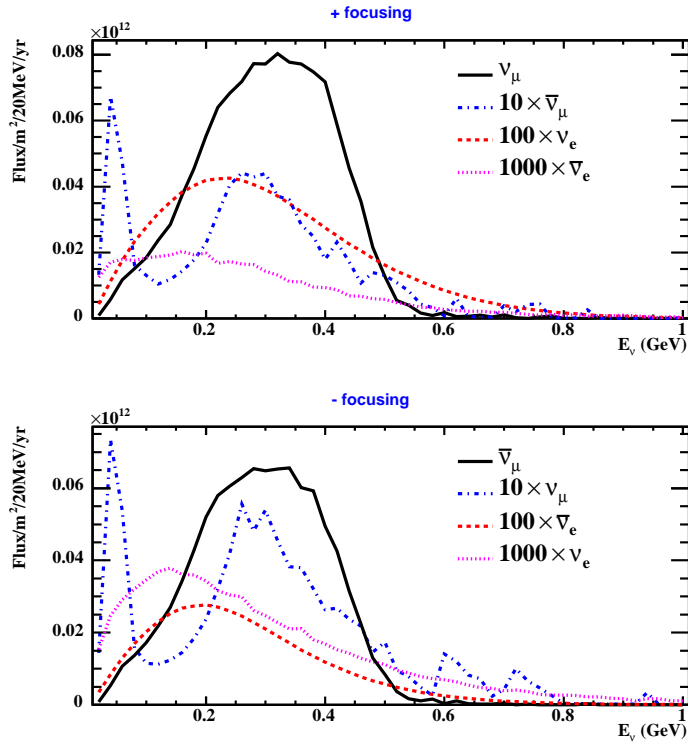


**Figure 2:** Neutrino fluxes, at 130 km from the target with the horns focusing the positive particles (top panel) or the negative particles (bottom panel). The fluxes are computed for a SPL proton beam of 3.5 GeV (4 MW), a decay tunnel with a length of 40 m and a radius of 2 m.

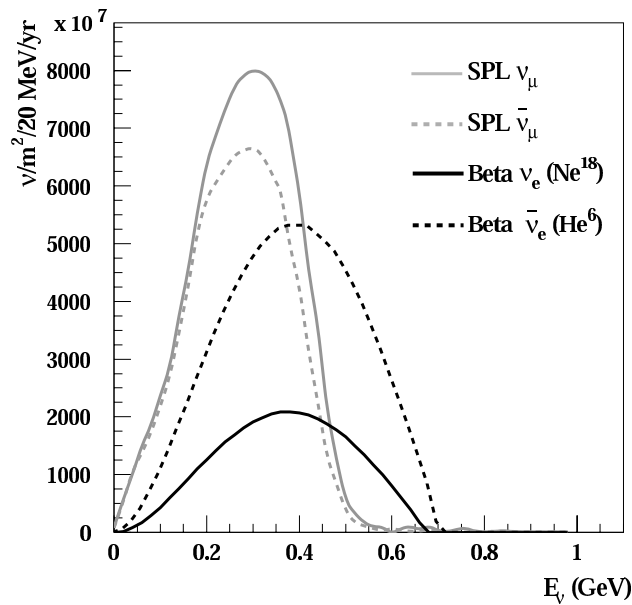


**Figure 3:** Comparison of the fluxes from SPL and  $\beta$ B.

and 2% miss identified muons from  $\bar{\nu}_\mu \rightarrow \bar{\nu}_\mu$  CC.

Considering the signal over square-root of background ratio, the 3.5 GeV beam energy is more favorable than the original 2.2 GeV option. Compared to the fluxes used in Refs. [35,49]

the gain is at least a factor 2.5 and this justifies to reconsider in detail the physics potential of the SPL Super Beam. Both the appearance and the disappearance channels are used. For the spectral analysis we use five bins of 200 MeV in the interval  $0 < E_\nu < 1$  GeV, adopting a Gaussian energy resolution with a constant width of 85 MeV to take into account the Fermi motion constraint in the energy reconstruction of QE events. As ultimate goal suggested in Ref. [15] a 2% systematical error is used as default both for signal and background, this would be achieved by a special care of the design of the close position. However, we discuss also how a 5% systematical error affects the sensitivities. Using neutrino cross-sections on water from Ref. [32], the number of expected  $\nu_\mu$  charged current is about 95 per kt yr. In Fig. 3 we compare the fluxes from the SPL to the one from the  $\beta$ B.

## 4 Degeneracies

A characteristic feature in the analysis of future LBL experiments is the presence of *parameter degeneracies*. Due to the inherent three-flavor structure of the oscillation probabilities, for a given experiment in general several disconnected regions in the multi-dimensional space of oscillation parameters will be present. Traditionally these degeneracies are referred to in the following way:

- The *intrinsic* or  $(\delta_{\text{CP}}, \theta_{13})$ -degeneracy [50]: For a measurement based on the  $\nu_\mu \rightarrow \nu_e$  oscillation probability for neutrinos and antineutrinos two disconnected solutions appear in the  $(\delta_{\text{CP}}, \theta_{13})$  plane.
- The *hierarchy* or  $\text{sign}(\Delta m_{31}^2)$ -degeneracy [51]: The two solutions corresponding to the two signs of  $\Delta m_{31}^2$  appear in general at different values of  $\delta_{\text{CP}}$  and  $\theta_{13}$ .
- The *octant* or  $\theta_{23}$ -degeneracy [52]: Since LBL experiments are sensitive mainly to  $\sin^2 2\theta_{23}$  it is difficult to distinguish the two octants  $\theta_{23} < \pi/4$  and  $\theta_{23} > \pi/4$ . Again, the solutions corresponding to  $\theta_{23}$  and  $\pi/2 - \theta_{23}$  appear in general at different values of  $\delta_{\text{CP}}$  and  $\theta_{13}$ .

This leads to an eight-fold ambiguity in  $\theta_{13}$  and  $\delta_{\text{CP}}$  [53], and hence degeneracies provide a serious limitation for the determination of  $\theta_{13}$ ,  $\delta_{\text{CP}}$ , and the sign of  $\Delta m_{31}^2$ . Recent discussions of degeneracies can be found for example in Refs. [29, 31, 54, 55]; degeneracies in the context of CERN–Fréjus  $\beta$ B and SPL have been considered previously in Ref. [35]. In Fig. 4 we illustrate the effect of degeneracies for the  $\beta$ B, SPL, and T2HK experiments. Assuming the true parameter values  $\delta_{\text{CP}} = -0.85\pi$ ,  $\sin^2 2\theta_{13} = 0.03$ ,  $\sin^2 \theta_{23} = 0.6$  we show the allowed regions in the plane of  $\sin^2 2\theta_{13}$  and  $\delta_{\text{CP}}$  taking into account the solutions with the wrong hierarchy and the wrong octant of  $\theta_{23}$ .

As visible in Fig. 4 for the Super Beam experiments SPL and T2HK there is only a four-fold degeneracy related to  $\text{sign}(\Delta m_{31}^2)$  and the octant of  $\theta_{23}$ , whereas the intrinsic degeneracy can be resolved. Several pieces of information contribute to this effect, as we illustrate at the example of SPL in Fig. 5. The dashed curves in that figure show the allowed regions for only the appearance measurement (for neutrinos and antineutrinos) without spectral information, i.e., just a counting experiment. In this case the eight-fold degeneracy is present in its full beauty, and one finds two solutions (corresponding to the intrinsic degeneracy)

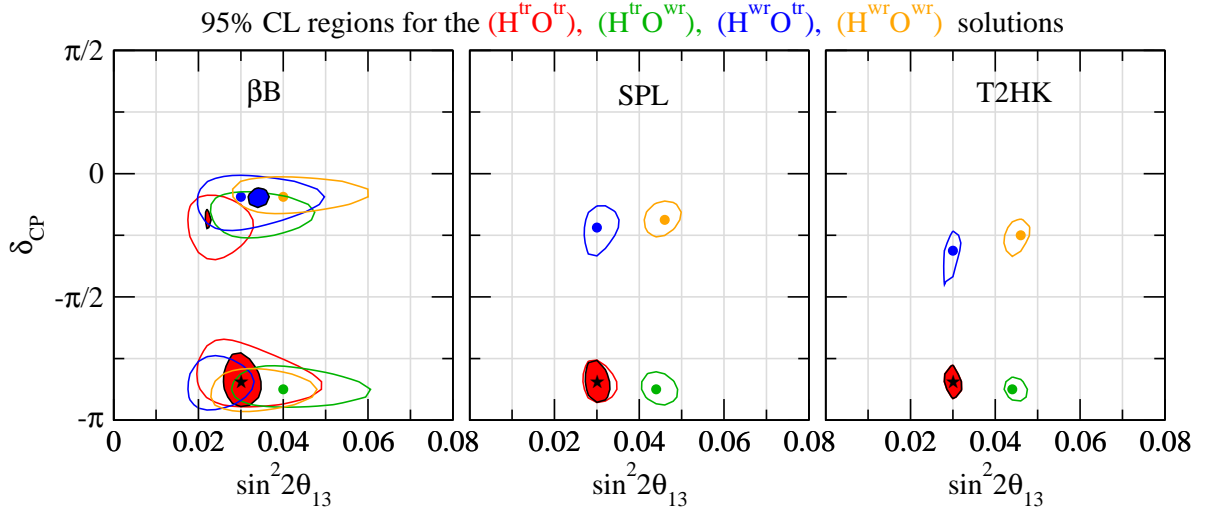


**Figure 4:** Allowed regions in  $\sin^2 2\theta_{13}$  and  $\delta_{\text{CP}}$  for LBL data alone (contour lines) and LBL+ATM data combined (colored regions).  $H^{\text{tr/wr}}(O^{\text{tr/wr}})$  refers to solutions with the true/wrong mass hierarchy (octant of  $\theta_{23}$ ). The true parameter values are  $\delta_{\text{CP}} = -0.85\pi$ ,  $\sin^2 2\theta_{13} = 0.03$ ,  $\sin^2 \theta_{23} = 0.6$ , and the values from Eq. (1) for the other parameters.

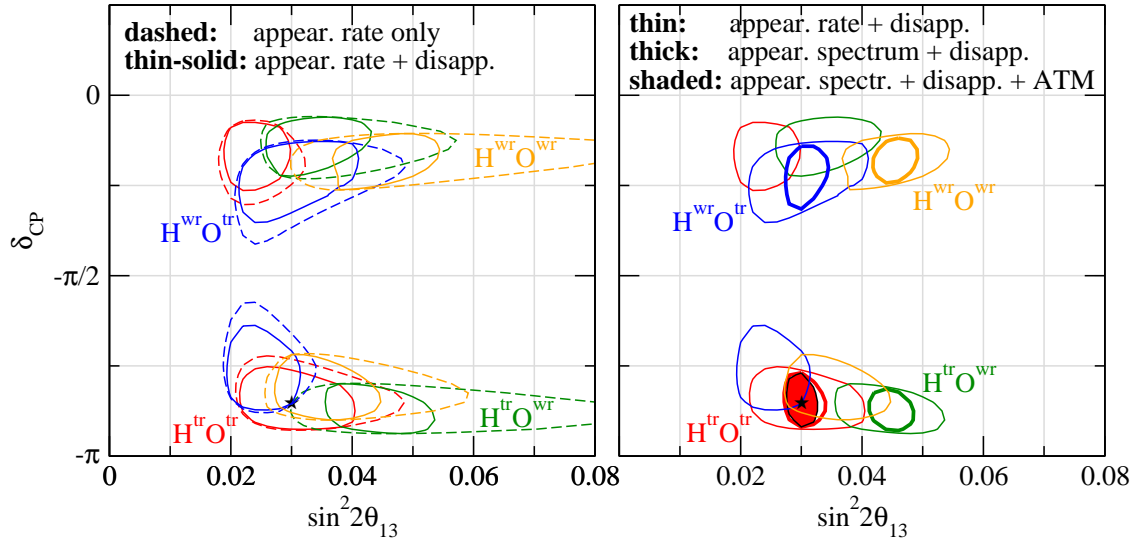


**Figure 5:** Resolving degeneracies in SPL by successively using the appearance rate measurement, disappearance channel, spectral information in the appearance channel, and atmospheric neutrinos. Allowed regions in  $\sin^2 2\theta_{13}$  and  $\delta_{\text{CP}}$  are shown at 95% CL, and  $H^{\text{tr/wr}}(O^{\text{tr/wr}})$  refers to solutions with the true/wrong mass hierarchy (octant of  $\theta_{23}$ ). The true parameter values are  $\delta_{\text{CP}} = -0.85\pi$ ,  $\sin^2 2\theta_{13} = 0.03$ ,  $\sin^2 \theta_{23} = 0.6$ , and the values from Eq. (1) for the other parameters.

for each choice of  $\text{sign}(\Delta m_{31}^2)$  and the octant of  $\theta_{23}$ . Moreover, the allowed regions are relatively large. For the thin solid curves the information from the disappearance channel is added. The main effect is to decrease the size of the allowed regions in  $\sin^2 2\theta_{13}$ . This is especially pronounced for the solutions involving the wrong octant of  $\theta_{23}$ , since these solutions are strongly affected by an uncertainty in  $\theta_{23}$  which gets reduced by the disappearance information. The most relevant effect comes from the inclusion of spectral information, as

visible from the comparison of the thin and thick curves in the right panel of Fig. 5. The intrinsic degeneracy gets resolved and only four solutions corresponding to the sign and octant degeneracies are left. Moreover, the size of the allowed regions in  $\sin^2 2\theta_{13}$  becomes again significantly smaller.<sup>2</sup> Note that the thin solid curves in the left and right panels are identical, and the thick curves in the right panel of Fig. 5 correspond to the regions show in Fig. 4 for the SPL. Finally, by the inclusion of information from atmospheric neutrinos all degeneracies can be resolved in this example, and the true solution is identified at 95% CL (see Sec. 6.2 and Ref. [29] for further discussions of atmospheric neutrinos).

Concerning the  $\beta$ B one observes from Fig. 4 that in this case the  $(\delta_{\text{CP}}, \theta_{13})$ -degeneracy cannot be resolved and one has to deal with eight distinct solutions. One reason for this is the absence of precise information on  $|\Delta m_{31}^2|$  and  $\sin^2 2\theta_{23}$  which is provided by the  $\nu_\mu$  disappearance in Super Beam experiments but is not available from the  $\beta$ B. If external information on these parameters at the level of 3% is included the allowed regions in Fig. 4 are significantly reduced. However, still all eight solutions are present, which indicates that for the  $\beta$ B spectral information is not efficient enough to resolve the  $(\delta_{\text{CP}}, \theta_{13})$ -degeneracy, and in this case only the inclusion of atmospheric neutrino data allows a nearly complete resolution of the degeneracies.

An important observation from Fig. 4 is that degeneracies have only a very small impact on the CP violation discovery, in the sense that if the true solution is CP violating also the fake solutions are located at CP violating values of  $\delta_{\text{CP}}$ . Indeed, since for the relatively short baselines in the experiments under consideration matter effects are very small, the  $\text{sign}(\Delta m_{31}^2)$ -degenerate solution is located within good approximation at  $\delta'_{\text{CP}} \approx \pi - \delta_{\text{CP}}$  [51]. Therefore, although degeneracies strongly affect the determination of  $\theta_{13}$  and  $\delta_{\text{CP}}$  they have only a small impact on the CP violation discovery potential. Furthermore, as clear from Fig. 4 the  $\text{sign}(\Delta m_{31}^2)$  degeneracy has practically no effect on the  $\theta_{13}$  measurement, whereas the octant degeneracy has very little impact on the determination of  $\delta_{\text{CP}}$ .

Fig. 4 shows also that the fake solutions occur at similar locations in the  $(\sin^2 2\theta_{13}, \delta_{\text{CP}})$  plane for  $\beta$ B and SPL. Therefore, as noted in Ref. [35], in this sense the two experiments are not complementary, and the combination of 10 years of  $\beta$ B and SPL data is not very effective in resolving degeneracies. This is obvious since the baseline is the same and the neutrino energies are similar. Note however, that the  $\beta$ B looks for  $\nu_e \rightarrow \nu_\mu$  appearance, whereas in SPL the T-conjugate channel  $\nu_\mu \rightarrow \nu_e$  is observed. Assuming CPT invariance the relation  $P_{\nu_\alpha \rightarrow \nu_\beta} = P_{\bar{\nu}_\beta \rightarrow \bar{\nu}_\alpha}$  holds, which implies that the antineutrino measurement can be replaced by a measurement in the T-conjugate channel. Hence, if  $\beta$ B and SPL experiments are available simultaneously the full information can be obtained just from neutrino data, and in principle the (time consuming) antineutrino measurement is not necessary. As shown in Fig. 6 the combination of 5 yrs neutrino data from the  $\beta$ B with 5 yrs of neutrino data from SPL leads to a result very close to the 10 yrs neutrino+antineutrino data from one experiment alone. Hence, if  $\beta$ B and SPL experiments are available simultaneously the data taking period is reduced approximately by a factor of 2 with respect to a single experiment. This synergy is discussed later in Sec. 6.1 in the context of the  $\theta_{13}$  and CP violation discovery potentials.

---

<sup>2</sup>The inclusion of spectral information might be the source of possible differences to previous studies, see e.g. Ref. [35].

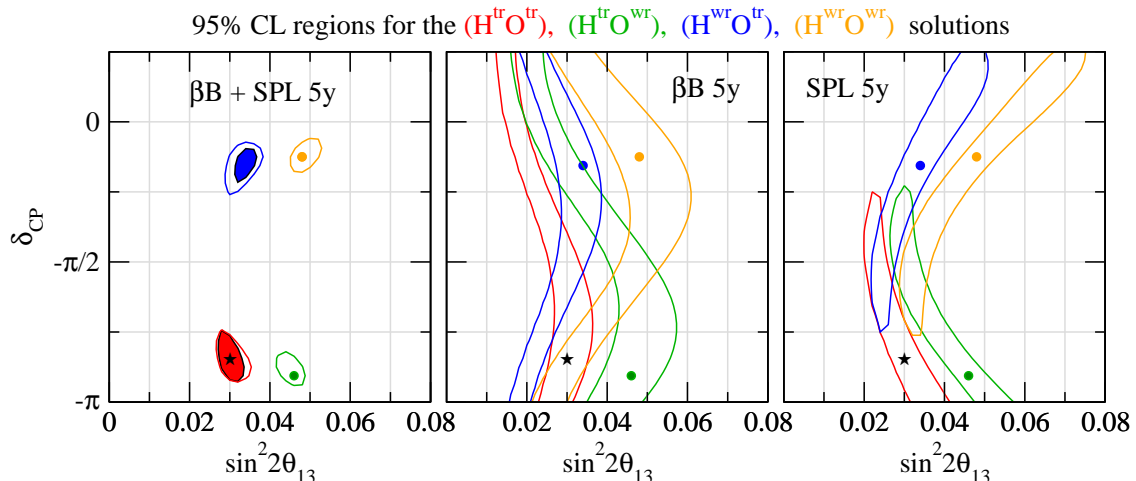


**Figure 6:** Allowed regions in  $\sin^2 2\theta_{13}$  and  $\delta_{\text{CP}}$  for 5 years data (neutrinos only) from  $\beta\text{B}$ , SPL, and the combination.  $\text{H}^{\text{tr/wr}}(\text{O}^{\text{tr/wr}})$  refers to solutions with the true/wrong mass hierarchy (octant of  $\theta_{23}$ ). For the colored regions in the left panel also 5 years of atmospheric data are included; the solution with the wrong hierarchy has  $\Delta\chi^2 = 3.3$ . The true parameter values are  $\delta_{\text{CP}} = -0.85\pi$ ,  $\sin^2 2\theta_{13} = 0.03$ ,  $\sin^2 \theta_{23} = 0.6$ , and the values from Eq. (1) for the other parameters. For the  $\beta\text{B}$  only analysis (middle panel) an external accuracy of 2% (3%) for  $|\Delta m_{31}^2|$  ( $\theta_{23}$ ) has been assumed, whereas for the left and right panel the default value of 10% has been used.

## 5 Physics potential

### 5.1 Sensitivity to the atmospheric parameters

The  $\nu_\mu$  disappearance channel available in the Super Beam experiments SPL and T2HK allows a precise determination of the atmospheric parameters  $|\Delta m_{31}^2|$  and  $\sin^2 2\theta_{23}$ , see, e.g., Refs. [56–58] for recent analyses). Fig. 7 illustrates the improvement on these parameters by Super Beam experiments with respect to the present knowledge from SK atmospheric and K2K data. We show the allowed regions at 99% CL for T2K-I, SPL, and T2HK, where in all three cases 5 years of neutrino data are assumed. T2K-I corresponds to the phase I of the T2K experiment with a beam power of 0.77 MW and the Super-Kamiokande detector as target [15]. In Tab. 4 we give the corresponding relative accuracies at  $3\sigma$  for  $|\Delta m_{31}^2|$  and  $\sin^2 \theta_{23}$ .

From the figure and the table it becomes evident that the T2K setups are very good in measuring the atmospheric parameters, and only a modest improvement is possible with SPL with respect to T2K phase I. T2HK provides an excellent sensitivity for these parameters, and for the example of the test point 2 sub-percent accuracies are obtained at  $3\sigma$ . The disadvantage of SPL with respect to T2HK is the limited spectral information. Because of the lower beam energy nuclear Fermi motion is a severe limitation for energy reconstruction in SPL, whereas in T2K the somewhat higher energy allows an efficient use of spectral information of quasi-elastic events. Indeed, due to the large number of events in the disappearance channel (cf. Tab. 2) the measurement is completely dominated by the spectrum, and even increasing the normalization uncertainty up to 100% has very little impact on the allowed regions. The effect of spectral information on the disappearance measurement is discussed

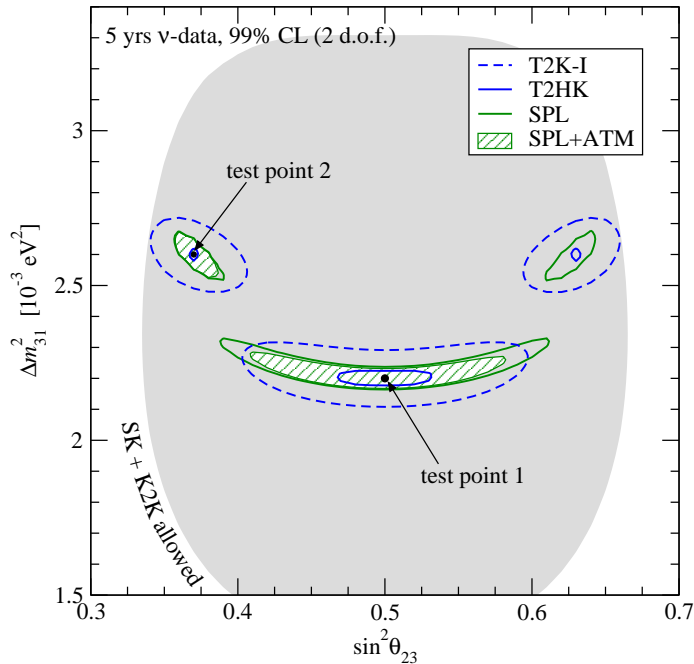


**Figure 7:** Allowed regions of  $\Delta m_{31}^2$  and  $\sin^2 \theta_{23}$  at 99% CL (2 d.o.f.) after 5 yrs of neutrino data taking for SPL, T2K phase I, T2HK, and the combination of SPL with 5 yrs of atmospheric neutrino data in the MEMPHYS detector. For the true parameter values we use  $\Delta m_{31}^2 = 2.2$  ( $2.6$ )  $\times 10^{-3}$  eV<sup>2</sup> and  $\sin^2 \theta_{23} = 0.5$  ( $0.37$ ) for the test point 1 (2), and  $\theta_{13} = 0$  and the solar parameters as given in Eq. (1). The shaded region corresponds to the 99% CL region from present SK and K2K data [11].

	True values	T2K-I	SPL	T2HK
$\Delta m_{31}^2$	$2.2 \cdot 10^{-3}$ eV <sup>2</sup>	4.7%	3.9%	1.1%
$\sin^2 \theta_{23}$	0.5	20%	22%	6%
$\Delta m_{31}^2$	$2.6 \cdot 10^{-3}$ eV <sup>2</sup>	4.4%	3.0%	0.7%
$\sin^2 \theta_{23}$	0.37	8.9%	4.7%	0.8%

**Table 4:** Accuracies at  $3\sigma$  on the atmospheric parameters  $|\Delta m_{31}^2|$  and  $\sin^2 \theta_{23}$  for 5 years of neutrino data from T2K-I, SPL, and T2HK for the two test points shown in Fig. 7 ( $\theta_{13}^{\text{true}} = 0$ ). The accuracy for a parameter  $x$  is defined as  $(x^{\text{upper}} - x^{\text{lower}})/(2x^{\text{true}})$ , where  $x^{\text{upper}}$  ( $x^{\text{lower}}$ ) is the upper (lower) bound at  $3\sigma$  for 1 d.o.f. obtained by projecting the contour  $\Delta\chi^2 = 9$  onto the  $x$ -axis. For the accuracies for test point 2 the octant degenerate solution is neglected.

in some detail in Ref. [58].

For the test point 1, with maximal mixing for  $\theta_{23}$ , rather poor accuracies of  $\sim 20\%$  for T2K-I and SPL, and 6% for T2HK are obtained for  $\sin^2 \theta_{23}$ . The reason is that in the disappearance channel  $\sin^2 2\theta_{23}$  is measured with high precision, which translates to rather large errors for  $\sin^2 \theta_{23}$  if  $\theta_{23} = \pi/4$  [57]. For the same reason it is difficult to resolve the octant degeneracy, and for the test point 2, with a non-maximal value of  $\sin^2 \theta_{23} = 0.37$ , for all three LBL experiments the degenerate solution is present around  $\sin^2 \theta_{23} = 0.63$ . As pointed out in Refs. [59, 60] atmospheric neutrino data may allow to distinguish between the two octants of  $\theta_{23}$ . If 5 years of atmospheric neutrino data in MEMPHYS are added to

### 3 $\sigma$ discovery of a non-zero $\theta_{13}$

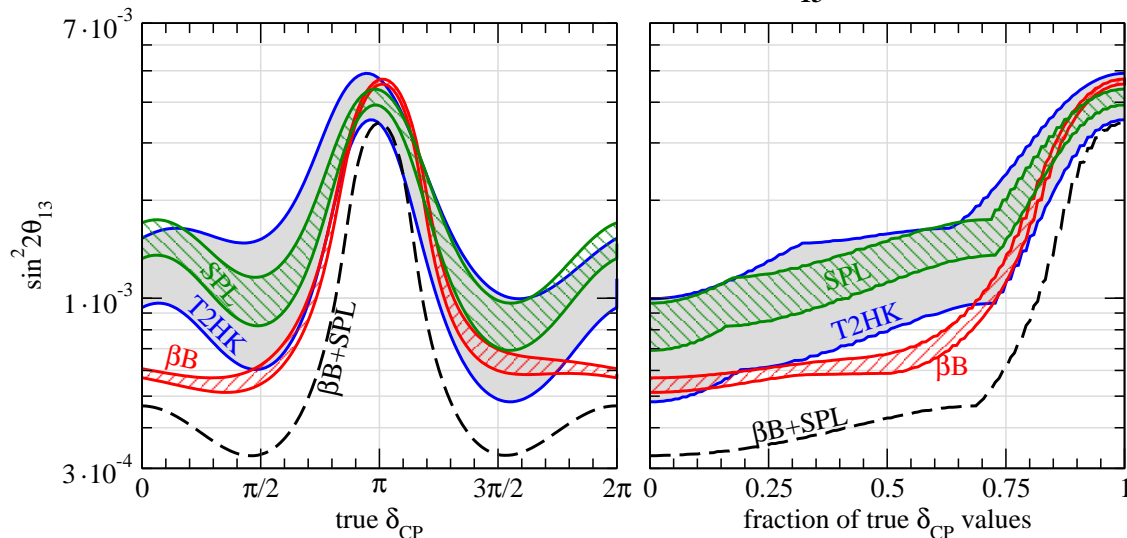


**Figure 8:**  $3\sigma$  discovery sensitivity to  $\sin^2 2\theta_{13}$  for  $\beta B$ , SPL, and T2HK as a function of the true value of  $\delta_{CP}$  (left panel) and as a function of the fraction of all possible values of  $\delta_{CP}$  (right panel). The width of the bands corresponds to values for the systematical errors between 2% and 5%. The dashed curves correspond to the combination of  $\beta B$  and SPL with 10 yrs of total data taking each for a systematical error of 2%.

the SPL data, the degenerate solution for the test point 2 can be excluded at more than  $5\sigma$  and hence the octant degeneracy is resolved in this example, see Sec. 6.2 for a more detailed discussion.

## 5.2 The $\theta_{13}$ discovery potential

If no finite value of  $\theta_{13}$  is discovered by the next round of experiments an important task of the experiments under consideration here is to push further the sensitivity to this parameter. In this section we address this problem, where we use the following definition of the  $\theta_{13}$  discovery potential: Data are simulated for a finite true value of  $\sin^2 2\theta_{13}$  and a given true value for  $\delta_{CP}$ . If the  $\Delta\chi^2$  of the fit to these data with  $\theta_{13} = 0$  is larger than 9 the corresponding true value of  $\theta_{13}$  “is discovered at  $3\sigma$ ”. In other words, the  $3\sigma$  discovery limit as a function of the true  $\delta_{CP}$  is given by the true value of  $\sin^2 2\theta_{13}$  for which  $\Delta\chi^2(\theta_{13} = 0) = 9$ . In the fitting process we minimize the  $\Delta\chi^2$  with respect to  $\theta_{12}$ ,  $\theta_{23}$ ,  $\Delta m_{12}^2$ , and  $\Delta m_{31}^2$ , and in general one has to test also for degenerate solutions in  $\text{sign}(\Delta m_{31}^2)$  and the octant of  $\theta_{23}$ .

The discovery limits are shown for  $\beta B$ , SPL, and T2HK in Fig. 8. One observes that the three facilities are rather similar in performance, and a guaranteed discovery reach of  $\sin^2 2\theta_{13} \simeq 5 \times 10^{-3}$  is obtained, irrespective of the actual value of  $\delta_{CP}$ . For certain values of  $\delta_{CP}$  the sensitivity is significantly improved, and the discovery limits below  $\sin^2 2\theta_{13} \simeq 10^{-3}$  are possible for a large fraction of all possible values of  $\delta_{CP}$  for all three facilities. In the most favorable case sensitivities of  $\sin^2 2\theta_{13} \simeq 5 (7) \times 10^{-4}$  can be reached for  $\beta B$  and T2HK (SPL), assuming systematical errors of 2%. If 10 years of data from  $\beta B$  and SPL are combined a discovery limit below  $\sin^2 2\theta_{13} = 4 \times 10^{-4}$  is reached for 45% of all possible values of  $\delta_{CP}$ .

In Fig. 8 we illustrate also the effect of systematical errors on the  $\theta_{13}$  discovery reach. The lower boundary of the band for each experiment corresponds to a systematical error of

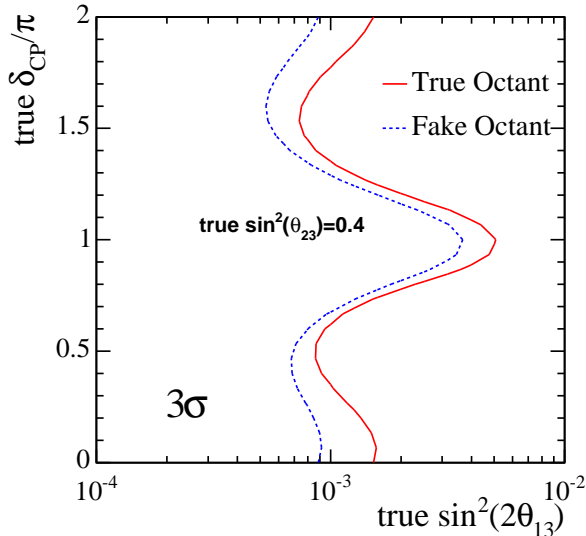


**Figure 9:**  $3\sigma$  discovery sensitivity to  $\sin^2 2\theta_{13}$  for the SPL as a function of the true value of  $\delta_{\text{CP}}$  for  $\sin^2 \theta_{23}^{\text{true}} = 0.4$  and true values for the other parameters as given in Eq. (1).

2%, whereas the upper boundary is obtained for 5%. These errors include the (uncorrelated) normalization uncertainties on the signal as well as on the background, where the crucial uncertainty is the error on the background. The fact that T2HK is relatively strongly affected by the actual value of the systematics can be understood by considering the ratio of signal to the square-root of the background using the numbers of Tab. 2. We shall discuss this issue in more detail in the next section in the context of the CP violation discovery reach.

Let us remark that the  $\theta_{13}$  sensitivities are practically not affected by the  $\text{sign}(\Delta m_{31}^2)$ -degeneracy. This is easy to understand, since the data is fitted with  $\theta_{13} = 0$ , and in this case both mass hierarchies lead to very similar event rates. If the inverted hierarchy is used as the true hierarchy, the peak in the discovery limit visible in the left panel of Fig. 8 around  $\delta_{\text{CP}} \sim \pi$  moves to  $\delta_{\text{CP}} \sim 0$ . However, the characteristic shape of the curves, and in particular, the sensitivity as a function of the  $\delta_{\text{CP}}$ -fraction shown in the right panel are hardly affected by the sign of the true  $\Delta m_{31}^2$ . In case of a non-maximal value of  $\theta_{23}$  the octant-degeneracy has a minor impact on the  $\theta_{13}$  discovery potential, as illustrated in Fig. 9 for the SPL. We show the discovery limit obtained with the true and the fake octant of  $\theta_{23}$  for a true value of  $\sin^2 \theta_{23} = 0.4$ . The size of the effect of a true value with  $\sin^2 \theta_{23} > 0.5$  is comparable.

### 5.3 Sensitivity to CP violation

In case a finite value of  $\theta_{13}$  is established it is important to quantitatively assess the discovery potential for leptonic CP violation (CPV). The CP symmetry is violated if the complex phase  $\delta_{\text{CP}}$  is different from 0 and  $\pi$ . Therefore, CPV is discovered if these values for  $\delta_{\text{CP}}$  can be excluded. We evaluate the discovery potential for CPV in the following way: Data are calculated by scanning the true values of  $\sin^2 2\theta_{13}$  and  $\delta_{\text{CP}}$ . Then these data are fitted with the CP conserving values  $\delta_{\text{CP}} = 0$  and  $\delta_{\text{CP}} = \pi$ , where all parameters except  $\delta_{\text{CP}}$  are varied and the sign and octant degeneracies are taken into account. If no fit with  $\Delta\chi^2 < 9$  is

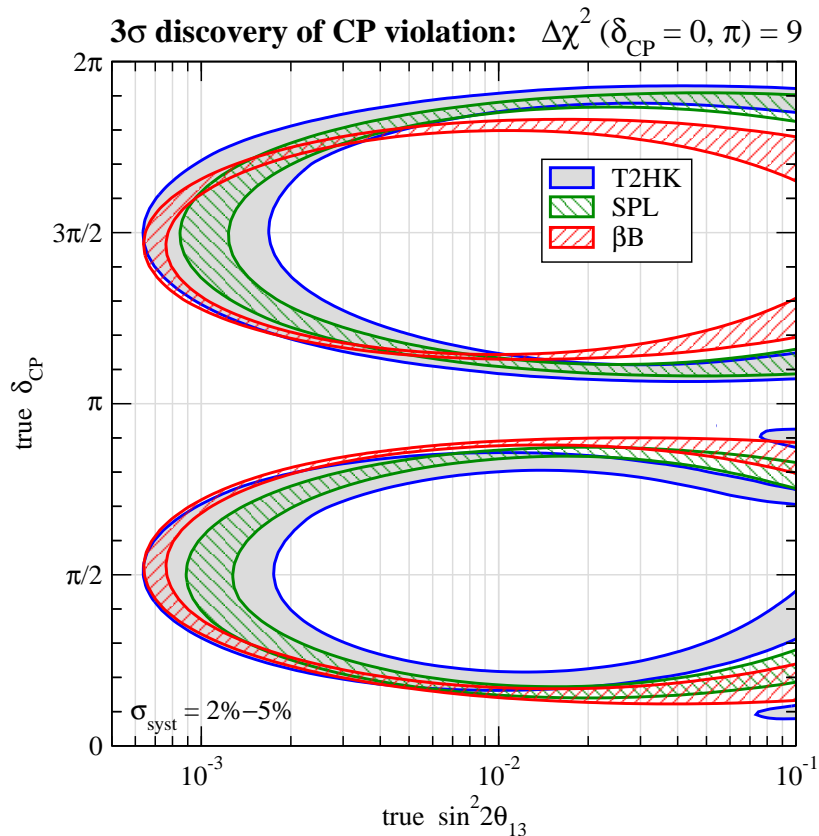


**Figure 10:** CPV discovery potential for  $\beta\text{B}$ , SPL, and T2HK: For parameter values inside the ellipse-shaped curves CP conserving values of  $\delta_{\text{CP}}$  can be excluded at  $3\sigma$  ( $\Delta\chi^2 > 9$ ). The width of the bands corresponds to values for the systematical errors from 2% to 5%.

found CP conserving values of  $\delta_{\text{CP}}$  can be excluded at  $3\sigma$  for the chosen values of  $\delta_{\text{CP}}^{\text{true}}$  and  $\sin^2 2\theta_{13}^{\text{true}}$ .

The CPV discovery potential for  $\beta\text{B}$ , SPL, and T2HK is shown in Fig. 10. As in the case of the  $\theta_{13}$  sensitivity we find that the three facilities perform rather similar. For systematical errors of 2% maximal CPV (for  $\delta_{\text{CP}}^{\text{true}} = \pi/2, 3\pi/2$ ) can be discovered at  $3\sigma$  down to  $\sin^2 2\theta_{13} \simeq 6 \times 10^{-4}$  for  $\beta\text{B}$  and T2HK, and  $\sin^2 2\theta_{13} \simeq 8 \times 10^{-4}$  for SPL, whereas the best sensitivity to CPV is obtained for  $\sin^2 2\theta_{13} \gtrsim 10^{-2}$ . For this value CPV can be established for 73%, 75%, 76% of all values of  $\delta_{\text{CP}}$  for  $\beta\text{B}$ , SPL, T2HK, respectively (again for systematics of 2%). The widths of the bands in Fig. 10 corresponds to different values for systematical errors. The curves which give the best sensitivities are obtained for systematics of 2%, the curves corresponding to the worst sensitivity have been computed for systematics of 5%. We find that for the SPL and especially for the  $\beta\text{B}$  systematics have a rather small impact on the CPV sensitivity, whereas T2HK is strongly affected.

This interesting feature can be understood in the following way. A rough measure to estimate the sensitivity is given by the signal compared to the error on the background. The latter receives contributions from the statistical error  $\sqrt{B}$  and from the systematical uncertainty  $\sigma_{\text{bkg}}B$ , where  $B$  is the number of background events and  $\sigma_{\text{bkg}}$  is the (relative) systematical error. Hence the importance of the systematics can be estimated by the ratio of systematical and statistical errors  $\sigma_{\text{bkg}}B/\sqrt{B} = \sigma_{\text{bkg}}\sqrt{B}$ . Summing the numbers for

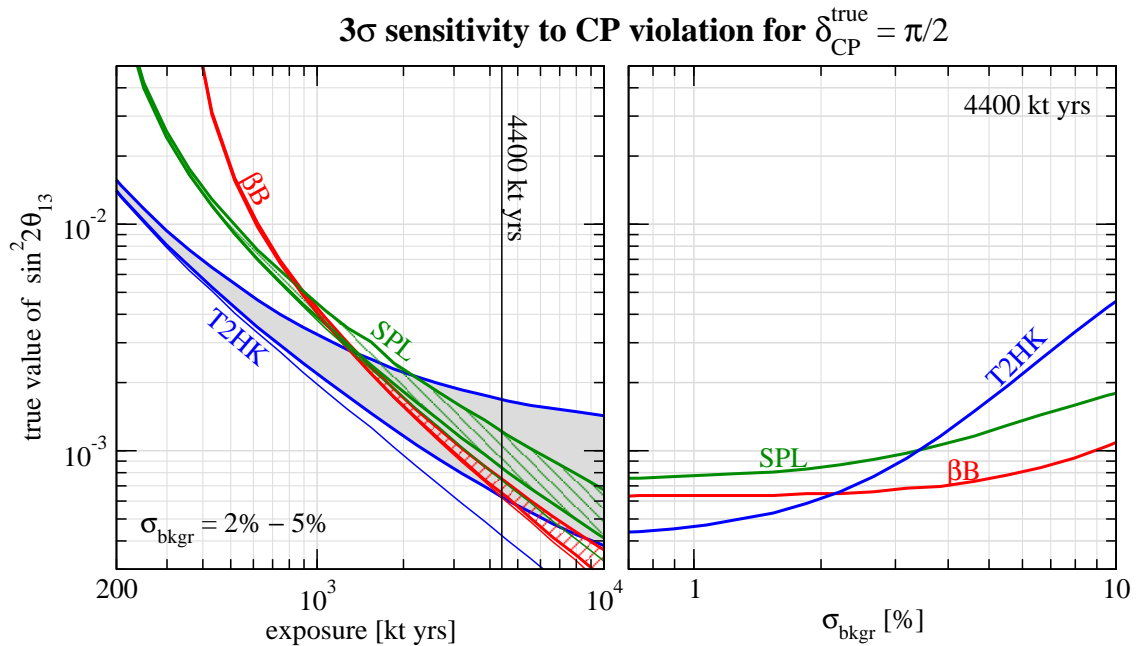


**Figure 11:** Impact of total exposure and systematical errors on the CPV discovery potential of  $\beta\text{B}$ , SPL, and T2HK. We show the smallest true value of  $\sin^2 2\theta_{13}$  for which  $\delta_{\text{CP}} = \pi/2$  can be distinguished from  $\delta_{\text{CP}} = 0$  or  $\delta_{\text{CP}} = \pi$  at  $3\sigma$  ( $\Delta\chi^2 > 9$ ) as a function of the exposure in kt yrs (left) and as a function of the systematical error on the background  $\sigma_{\text{bkgr}}$  (right). The widths of the curves in the left panel corresponds to values of  $\sigma_{\text{bkgr}}$  from 2% to 5%. The thin solid curves in the left panel corresponds to no systematical errors. The right plot is calculated for the standard exposure of 4400 kt yrs. No systematical error on the signal has been assumed.

background events in the neutrino and antineutrino channels given in Tab. 2 one finds that systematical errors dominate ( $\sigma_{\text{bkgr}}\sqrt{B} > 1$ ) if  $\sigma_{\text{bkgr}} \gtrsim 6\%$ ,  $3\%$ ,  $2\%$  for  $\beta\text{B}$ , SPL, T2HK, respectively.

In the right panel Fig. 11 we show the sensitivity to maximal CPV (as defined in the figure caption) as a function of  $\sigma_{\text{bkgr}}$ . Indeed, the worsening of the sensitivity due to systematics occurs roughly at the values of  $\sigma_{\text{bkgr}}$  as estimated above. More quantitatively the behavior of these curves can be understood from considering the number of signal and background events for neutrinos and antineutrinos. The curves for  $\beta\text{B}$  and T2HK can be reproduced rather accurately by a simple analytic  $\chi^2$ -function based on the total rates by using the numbers given Tab. 2. For SPL also spectral information is important, which indicates that in this case the spectrum of the background is rather different from the one of the signal of CPV.

The left panel of Fig. 11 shows the sensitivity to maximal CPV as a function of the exposure time for values of  $\sigma_{\text{bkgr}}$  from 2% to 5%. One can observe clearly that for the standard exposure of 4400 kt yrs T2HK is dominated by systematics and changing  $\sigma_{\text{bkgr}}$  from 2% to 5% has a big impact on the sensitivity. In contrast the CERN–MEMPHYS experiments are rather stable with respect to systematics and for the standard exposure they are still statistics dominated. We conclude that in T2HK systematics have to be under very good control<sup>3</sup>, whereas this issue is less important for  $\beta\text{B}$  and SPL. We have checked

<sup>3</sup>As a possible solution to this problem for T2HK it has been proposed in Ref. [55] to place one half of

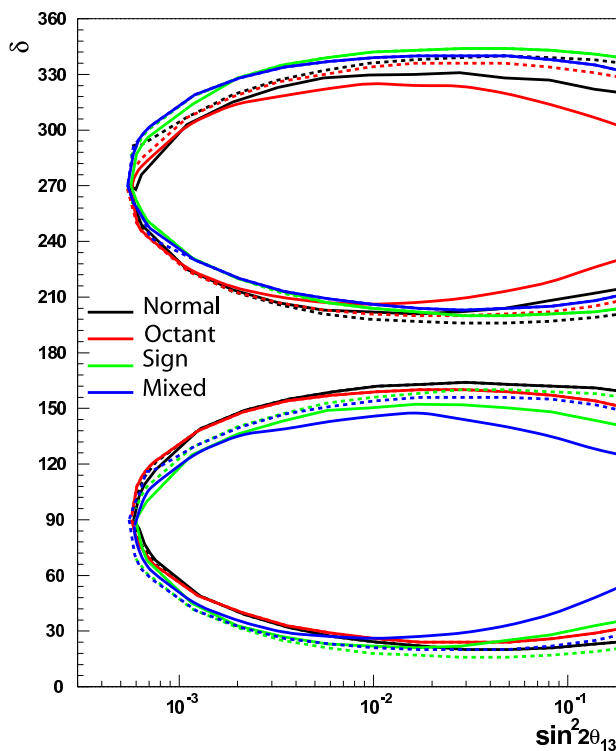


**Figure 12:** Impact of degeneracies on the CPV discovery potential for the  $\beta$ B. We show the sensitivity to CPV at  $3\sigma$  ( $\Delta\chi^2 > 9$ ) computed for 4 different options about the true parameter values: Normal:  $\text{sign}(\Delta m_{31}^2) = 1$ ,  $\theta_{23} = 40^\circ$ ; Octant:  $\text{sign}(\Delta m_{31}^2) = 1$ ,  $\theta_{23} = 60^\circ$ ; Sign:  $\text{sign}(\Delta m_{31}^2) = -1$ ,  $\theta_{23} = 40^\circ$ ; Mixed:  $\text{sign}(\Delta m_{31}^2) = -1$ ,  $\theta_{23} = 60^\circ$ . Dotted curves are computed neglecting degeneracies.

explicitly that the systematical error on the signal has negligible impact on these results. Therefore, we have set this error to zero for calculating Fig. 11 to highlight the importance of the background error. In all other calculations also the signal error is included, in particular also in Fig. 10.

Finally, in Fig. 12 we illustrate the impact of degeneracies, as well as the true hierarchy and  $\theta_{23}$ -octant on the CPV sensitivity. Curves of different colors correspond to the four different choices for  $\text{sign}(\Delta m_{31}^2)$  and the  $\theta_{23}$ -octant of the true parameters. For the solid curves the simulated data for each choice of true  $\text{sign}(\Delta m_{31}^2)$  and  $\theta_{23}$ -octant are fitted by taking into account all four degenerate solutions, i.e., also for the fit all four combinations of  $\text{sign}(\Delta m_{31}^2)$  and  $\theta_{23}$ -octant are used. One observes from the figure that the true hierarchy and octant have a rather small impact on the  $\beta$ B CPV sensitivity, in particular the sensitivity to maximal CPV is completely independent. The main effect of changing the true hierarchy is to exchange the behavior between  $0 < \delta_{\text{CP}} < 180^\circ$  and  $180^\circ < \delta_{\text{CP}} < 360^\circ$ . For  $\sin^2 2\theta_{13} \lesssim 10^{-2}$  the sensitivity gets slightly worse if  $\theta_{23}^{\text{true}} > \pi/4$  compared to  $\theta_{23}^{\text{true}} < \pi/4$ .

The dotted curves in Fig. 12 are computed without taking into account the degeneracies, i.e., for each choice of true  $\text{sign}(\Delta m_{31}^2)$  and  $\theta_{23}$ -octant the data are fitted only with this particular choice. The effect of the degeneracies becomes visible for large values of  $\theta_{13}$ . Note that this is just the region where they can be reduced by a combined analysis with atmospheric neutrinos (see Sec. 6.2 or Ref. [29]).

the Hyper-K detector mass at Kamioka and the second half at the same off-axis angle in Korea.

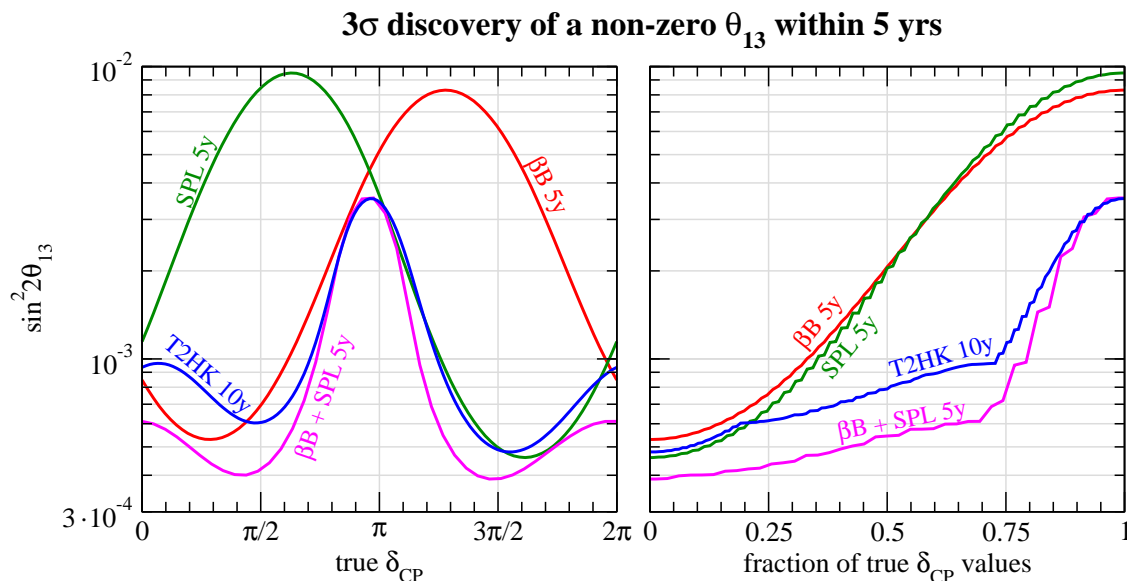


**Figure 13:** Discovery potential of a finite value of  $\sin^2 2\theta_{13}$  at  $3\sigma$  ( $\Delta\chi^2 > 9$ ) for 5 yrs neutrino data from  $\beta B$ , SPL, and the combination of  $\beta B + SPL$  compared to 10 yrs data from T2HK (2 yrs neutrinos + 8 yrs antineutrinos).

## 6 Synergies provided by the CERN–MEMPHYS facilities

### 6.1 Combining Beta Beam and Super Beam

In this section we discuss synergies which emerge if both  $\beta B$  and SPL are available. The main difference between these two beams is the different initial neutrino flavor,  $(\bar{\nu}_e)$  for  $\beta B$  and  $(\bar{\nu}_\mu)$  for SPL. This implies that at near detectors all relevant cross sections can be measured. In particular, the near detector of the  $\beta B$  will measure the cross section for the SPL appearance search, and vice versa. If both experiments run with neutrinos and antineutrinos all possible transition probabilities are covered:  $P_{\nu_e \rightarrow \nu_\mu}$ ,  $P_{\bar{\nu}_e \rightarrow \bar{\nu}_\mu}$ ,  $P_{\nu_\mu \rightarrow \nu_e}$ , and  $P_{\bar{\nu}_\mu \rightarrow \bar{\nu}_e}$ . Together with the fact that matter effects are very small because of the relatively short baseline, this means that in addition to CP also direct tests of the T and CPT symmetries are possible.

However, if the CPT symmetry is assumed in principle all information can be obtained just from neutrino data because of the relations  $P_{\bar{\nu}_e \rightarrow \bar{\nu}_\mu} = P_{\nu_\mu \rightarrow \nu_e}$  and  $P_{\bar{\nu}_\mu \rightarrow \bar{\nu}_e} = P_{\nu_e \rightarrow \nu_\mu}$ . As mentioned already in Sec. 4 this implies that (time consuming) antineutrino running can be avoided. We illustrate this synergy in Figs. 13 and 14. In Fig. 13 we show the  $\theta_{13}$  discovery potential of 5 years of neutrino data from  $\beta B$  and SPL. From the left panel the complementarity of the two experiments is obvious, since each of them is most sensitive in a different region of  $\delta_{CP}$ .<sup>4</sup> Combining these two data sets results in a sensitivity slightly better than from 10 years ( $2\nu + 8\bar{\nu}$ ) of T2HK data. As visible in Fig. 14 also for the CPV discovery this synergy works and 5 years of neutrino data from  $\beta B$  and SPL lead to a similar sensitivity as 10 years of T2HK.

<sup>4</sup>As expected from general properties of the oscillation probabilities the sensitivity curves of  $\beta B$  and SPL are approximately related by the transformation  $\delta_{CP} \rightarrow 2\pi - \delta_{CP}$ .

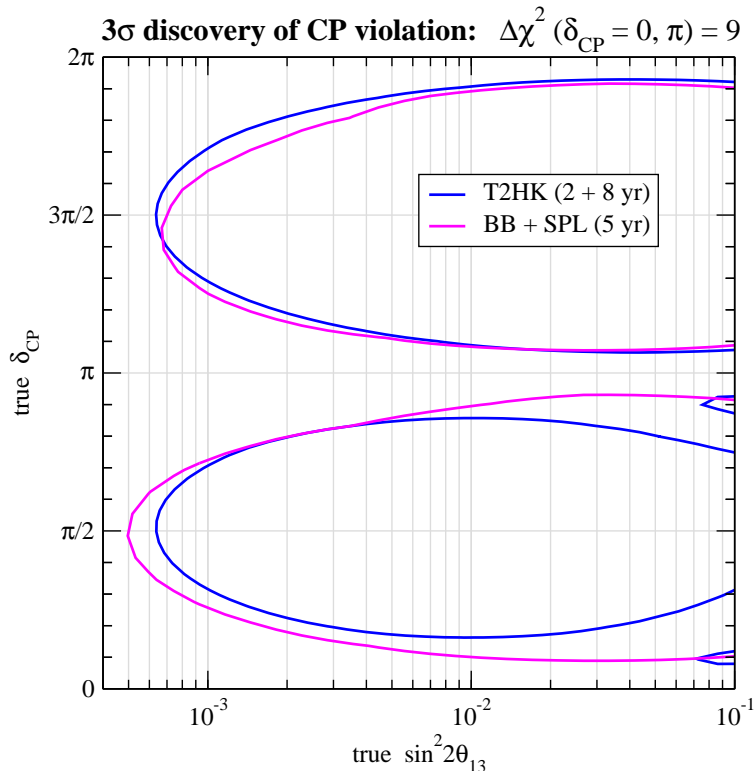


**Figure 14:** Sensitivity to CPV at  $3\sigma$  ( $\Delta\chi^2 > 9$ ) for combining 5 yrs neutrino data from  $\beta$ B and SPL compared to 10 yrs data from T2HK (2 yrs neutrinos + 8 yrs antineutrinos).

## 6.2 Resolving degeneracies with atmospheric neutrinos

It was pointed out in Ref. [29] that for LBL experiments based on mega ton scale water Čerenkov detectors data from atmospheric neutrinos (ATM) provide an attractive method to resolve degeneracies. Atmospheric neutrinos are sensitive to the neutrino mass hierarchy if  $\theta_{13}$  is sufficiently large due to Earth matter effects, mainly in multi-GeV  $e$ -like events [61–63]. Moreover, sub-GeV  $e$ -like events provide sensitivity to the octant of  $\theta_{23}$  [59, 60, 64] due to oscillations with  $\Delta m_{21}^2$  (see also Ref. [65] for a discussion of atmospheric neutrinos in the context of Hyper-K). Following Ref. [29] we investigate here the synergy from a combination of LBL data from  $\beta$ B and SPL with ATM data in the MEMPHYS detector. A general three-flavor analysis of ATM data is performed based on Ref. [60] and references therein. We include fully-contained  $e$ -like and  $\mu$ -like events (further divided into sub-GeV  $p_l < 400$  MeV, sub-GeV  $p_l > 400$  MeV, and Multi-GeV events), partially-contained  $\mu$ -like events, stopping muons, and through-going muons. Each of these data samples is divided into 10 zenith bins, so we have a total of 90 data points. The simulation of the atmospheric event rates has been adapted to the actual geometry of the MEMPHYS detector proposal (see Fig. 1). Details of the statistical analysis can be found in Ref. [66]. Note that our analysis of atmospheric data is conservative, since there is room for improvement by including multi-ring events as well as by optimizing the energy binning.<sup>5</sup>

The effect of degeneracies in LBL data has been discussed in Sec. 4, see Figs. 4 and 5.

<sup>5</sup>The impact of energy binning on the hierarchy determination with atmospheric neutrinos has been discussed recently in Ref. [67] in the context of magnetized iron detectors.

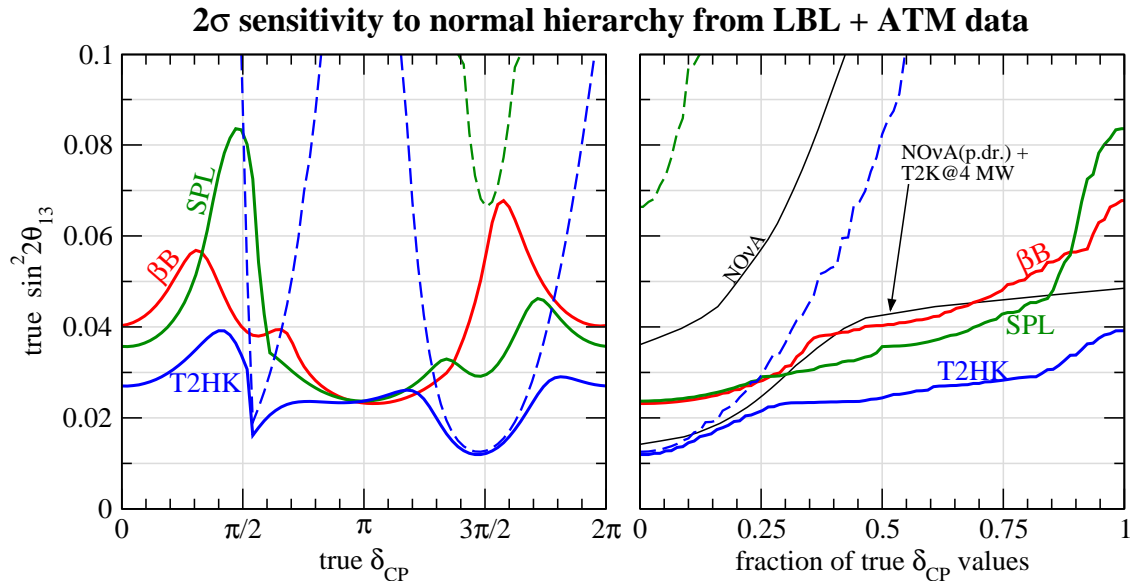


**Figure 15:** Sensitivity to the mass hierarchy at  $2\sigma$  ( $\Delta\chi^2 = 4$ ) as a function of the true values of  $\sin^2 2\theta_{13}$  and  $\delta_{\text{CP}}$  (left), and the fraction of true values of  $\delta_{\text{CP}}$  (right). The solid curves are the sensitivities from the combination of long-baseline and atmospheric neutrino data, the dashed curves correspond to long-baseline data only. For comparison we show in the right panel also the sensitivities of  $\text{NO}\nu\text{A}$  and  $\text{NO}\nu\text{A}+\text{T2K}$  extracted from Fig. 13.14 of Ref. [16]. For the curve labeled “ $\text{NO}\nu\text{A}$  (p.dr.)+ $\text{T2K}@4$  MW” a proton driver has been assumed for  $\text{NO}\nu\text{A}$  and the T2K beam has been up-graded to 4 MW, see Ref. [16] for details.

As discussed there, for given true parameter values the data can be fitted with the wrong hierarchy and/or with the wrong octant of  $\theta_{23}$ . Hence, from LBL data alone the hierarchy and the octant cannot be determined and ambiguities exist in the determination of  $\theta_{13}$  and  $\delta_{\text{CP}}$ . If the LBL data are combined with ATM data only the colored regions in Fig. 4 survive, i.e., in this particular example for SPL and T2HK the degeneracies are completely lifted at 95% CL, the mass hierarchy and the octant of  $\theta_{23}$  can be identified, and the ambiguities in  $\theta_{13}$  and  $\delta_{\text{CP}}$  are resolved. For the  $\beta\text{B}$  an island corresponding to the wrong hierarchy does survive at the 95% CL for 2 dof. Still, the solution with the wrong sign of  $\Delta m_{31}^2$  is disfavored with  $\Delta\chi^2 = 4.8$  with respect to the true solution, which corresponds to  $2.2\sigma$  for 1 dof. Let us note that in Fig. 4 we have chosen a favorable value of  $\sin^2 \theta_{23} = 0.6$ ; for values  $\sin^2 \theta_{23} < 0.5$  in general the sensitivity of ATM data is weaker [29].

In Fig. 15 we show how the combination of ATM+LBL data leads to a non-trivial sensitivity to the neutrino mass hierarchy, i.e. to the sign of  $\Delta m_{31}^2$ . For LBL data alone (dashed curves) there is practically no sensitivity for the CERN–MEMPHYS experiments (because of the very small matter effects due to the relatively short baseline), and the sensitivity of T2HK depends strongly on the true value of  $\delta_{\text{CP}}$ . However, by including data from atmospheric neutrinos (solid curves) the mass hierarchy can be identified at  $2\sigma$  CL provided  $\sin^2 2\theta_{13} \gtrsim 0.03 - 0.05$  for  $\beta\text{B}$  and SPL, and  $\sin^2 2\theta_{13} \gtrsim 0.02 - 0.03$  for T2HK, where for the CERN experiments the sensitivity shows somewhat more dependence on the true value of  $\delta_{\text{CP}}$ . As an example we have chosen in that figure a true value of  $\theta_{23} = \pi/4$ . Generically the hierarchy sensitivity increases with increasing  $\theta_{23}$ , see Ref. [29] for a detailed discussion.

For comparison we show in the right panel of Fig. 15 also the sensitivity of the  $\text{NO}\nu\text{A}$  [16] experiment, and of  $\text{NO}\nu\text{A}+\text{T2K}$ , where in the second case a beam upgrade by a proton driver

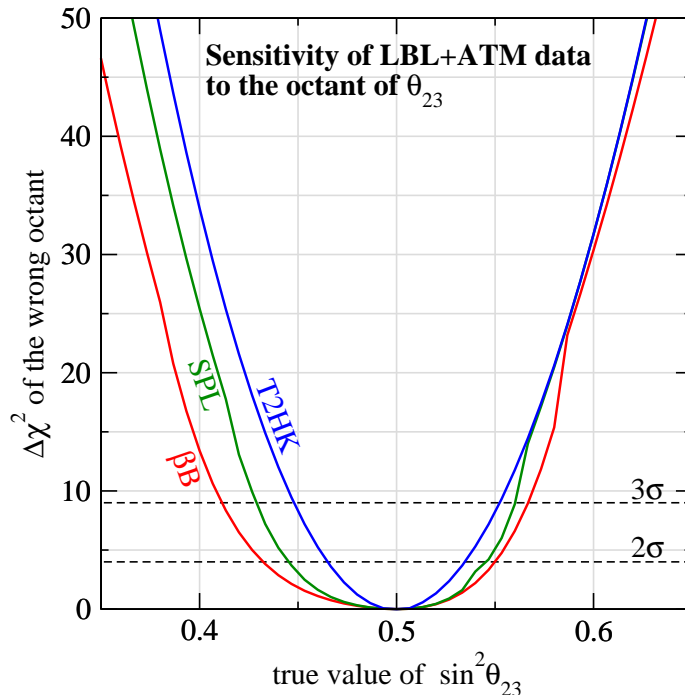


**Figure 16:**  $\Delta\chi^2$  of the solution with the wrong octant of  $\theta_{23}$  as a function of the true value of  $\sin^2\theta_{23}$ . We have assumed a true value of  $\theta_{13} = 0$ .

has been assumed for NO $\nu$ A, and for T2K the Super-Kamiokande detector has been used but the beam intensity has been increased by assuming 4 MW power. More details on these sensitivities can be found in Ref. [16]. Let us note that in general LBL experiments with two detectors (or the combination of two different LBL experiments) are a competitive method to atmospheric neutrinos for the hierarchy determination, see, e.g., Refs. [55, 68] for recent analyses. We mention also the possibility to determine the neutrino mass hierarchy by using neutrino events from a galactic Super Nova explosion in mega ton Čerenkov detectors such as MEMPHYS, see, e.g., Ref. [69].

Fig. 16 shows the potential of ATM+LBL data to exclude the octant degenerate solution. Since this effect is based mainly on oscillations with  $\Delta m_{21}^2$  there is very good sensitivity even for  $\theta_{13} = 0$ ; a finite value of  $\theta_{13}$  in general improves the sensitivity [29]. From the figure one can read off that  $\beta$ B, SPL, T2HK can resolve the correct octant at  $3\sigma$  if  $|\sin^2\theta_{23} - 0.5| \gtrsim 0.05, 0.07, 0.09$ , respectively. The improvement of the octant sensitivity with respect to previous analyses [29, 60] follows from changes in the analysis of sub-GeV atmospheric events, where now two bins in lepton momentum are used instead of one. It is interesting to note that though the  $\beta$ B has practically no sensitivity to  $\theta_{23}$  and the precision on  $\theta_{23}$  from the  $\beta$ B is very poor, together with atmospheric data it can provide non-trivial information on the octant.

## 7 Summary

In this work we have studied the physics potential of the CERN–MEMPHYS neutrino oscillation project. We consider a Beta Beam ( $\beta$ B) with  $\gamma = 100$  for the stored ions, where

existing facilities at CERN can be used optimally, and a Super Beam based on an optimized Super Proton Linac (SPL) with a beam energy of 3.5 GeV and 4 MW power. As target we assume the MEMPHYS detector, a 440 kt water Čerenkov detector at Fréjus, at a distance of 130 km from CERN. The main characteristics of the experiments are summarized in Tab. 1. The adopted neutrino fluxes are based on realistic calculations of ion production and storage for the  $\beta$ B, and a full simulation of the beam line (particle production and decay of secondaries) for SPL. Special care has been given to the issue of backgrounds, which we include by means of detailed event simulations and applying Super-Kamiokande particle identification algorithms.

The physics potential of the  $\beta$ B and SPL experiments in terms of  $\theta_{13}$  discovery reach and sensitivity to CP violation has been addressed where parameter degeneracies are fully taken into account. The main results on these performance indicators are summarized in Figs. 8 and 10. We obtain a guaranteed discovery reach of  $\sin^2 2\theta_{13} \simeq 5 \times 10^{-3}$  at  $3\sigma$ , irrespective of the actual value of  $\delta_{\text{CP}}$ . For certain values of  $\delta_{\text{CP}}$  the sensitivity is significantly improved, and discovery limits below  $\sin^2 2\theta_{13} \simeq 10^{-3}$  are possible for a large fraction of all possible values of  $\delta_{\text{CP}}$ . If 10 years of data from  $\beta$ B and SPL are combined a discovery limit below  $\sin^2 2\theta_{13} = 4 \times 10^{-4}$  is reached for 45% of all possible values of  $\delta_{\text{CP}}$ . Maximal CP violation (for  $\delta_{\text{CP}}^{\text{true}} = \pi/2, 3\pi/2$ ) can be discovered at  $3\sigma$  down to  $\sin^2 2\theta_{13} \simeq 6(8) \times 10^{-4}$  for  $\beta$ B (SPL), whereas the best sensitivity to CP violation is obtained for  $\sin^2 2\theta_{13} \gtrsim 10^{-2}$ . For this value CP violation can be established for 73% (75%) of all values of  $\delta_{\text{CP}}$  for  $\beta$ B (SPL). The impact of the value of systematical uncertainties on signal and background on these results is discussed. The  $\beta$ B and SPL sensitivities are compared to the ones of the phase II of the T2K experiment in Japan (T2HK), which is a competing proposal of similar size and timescale. In general we obtain rather similar sensitivities, and hence the CERN–MEMPHYS experiments provide a viable alternative to T2HK. We find that  $\beta$ B and SPL are less sensitive to systematical errors, whereas the sensitivity of T2HK crucially depends on the systematical error on the background.<sup>6</sup>

Assuming that both  $\beta$ B and SPL experiments are available, we point out that one can benefit from the different oscillation channels  $\nu_e \rightarrow \nu_\mu$  for  $\beta$ B and  $\nu_\mu \rightarrow \nu_e$  for SPL, since by the combination of these channels the time intensive antineutrino measurements can be avoided. We show that 5 years of neutrino data from  $\beta$ B and SPL lead to similar results as 2 years of neutrino plus 8 years of antineutrino data from T2HK. Furthermore, we discuss the use of atmospheric neutrinos in the MEMPHYS detector to resolve parameter degeneracies in the long-baseline data. This effect leads to a sensitivity to the neutrino mass hierarchy at  $2\sigma$  CL for  $\sin^2 2\theta_{13} \gtrsim 0.03 - 0.05$  for  $\beta$ B and SPL, although these experiments alone (without atmospheric data) have no sensitivity at all. Furthermore, the combination of atmospheric data with a Super Beam provides a possibility to determine the octant of  $\theta_{23}$ .

To conclude, we have shown that the CERN–MEMPHYS neutrino oscillation project based on a Beta Beam and/or a Super Beam plus a mega ton scale water Čerenkov detector offers interesting and competitive physics possibilities and is worth to be considered as a serious option in the worldwide process of identifying future high precision neutrino oscillation facilities [33].

---

<sup>6</sup>Let us note that in the present study we have not considered the recent “T2KK” proposal [55], where one half of the Hyper-K detector mass is at Kamioka and the second half in Korea. For such a setup our results do not apply and especially the conclusion on systematical errors may be different.

## Acknowledgment

We thank J. Argyriades for communication on the Super-K atmospheric neutrino analysis, A. Cazes for his work on the SPL simulation, and P. Huber for his patience in answering questions concerning the use of GLoBES. T.S. is supported by the 6<sup>th</sup> Framework Program of the European Community under a Marie Curie Intra-European Fellowship.

## References

- [1] B. T. Cleveland *et al.*, *Astrophys. J.* **496** (1998) 505; J.N. Abdurashitov *et al.* [SAGE], *J. Exp. Theor. Phys.* **95** (2002) 181 [astro-ph/0204245]; T. Kirsten *et al.* [GALLEX and GNO], *Nucl. Phys. B (Proc. Suppl.)* **118** (2003) 33; S. Fukuda *et al.* [Super-Kamiokande], *Phys. Lett.* **B539** (2002) 179; Q.R. Ahmad *et al.* [SNO], *Phys. Rev. Lett.* **89**, 011302 (2002) [nucl-ex/0204009]; B. Aharmim *et al.* [SNO], *Phys. Rev. C* **72** (2005) 055502 [nucl-ex/0502021].
- [2] Super-Kamiokande Coll., Y. Fukuda *et al.*, *Phys. Rev. Lett.* **81** (1998) 1562 [hep-ex/9807003]; Y. Ashie *et al.*, *Phys. Rev. D* **71**, 112005 (2005) [hep-ex/0501064].
- [3] T. Araki *et al.* [KamLAND Coll.], *Phys. Rev. Lett.* **94**, 081801 (2005) [hep-ex/0406035].
- [4] E. Aliu *et al.* [K2K Coll.], *Phys. Rev. Lett.* **94**, 081802 (2005) [hep-ex/0411038].
- [5] T. Thomson [MINOS Coll.], *Nucl. Phys. B (Proc. Suppl.)* **143**, 249 (2005); P. Adamson *et al.*, NuMi-L-337.
- [6] D. Autiero [OPERA Coll.], *Nucl. Phys. B (Proc. Suppl.)* **143**, 257 (2005); M. Guler *et al.*, *Experiment proposal*, CERN/SPSC 2000-028 SPSC/P318 LNGS P25/2000.
- [7] G. Acquistapace *et al.*, CERN-98-02.
- [8] A. Athanassopoulos *et al.*, *Phys. Rev. Lett.* **81**, 1774 (1998); A. Aguilar *et al.*, *Phys. Rev. D* **64**, 112007 (2001).
- [9] I. Stancu *et al.*, FERMILAB-TM-2207.
- [10] G. L. Fogli, E. Lisi, A. Marrone and A. Palazzo, hep-ph/0506083;
- [11] M. Maltoni, T. Schwetz, M. A. Tortola and J. W. F. Valle, *New J. Phys.* **6**, 122 (2004) [hep-ph/0405172]; T. Schwetz, *Acta Phys. Polon. B* **36**, 3203 (2005) [hep-ph/0510331].
- [12] B. Pontecorvo, *Sov. Phys.–JETP* **6**, 429 (1957) [*Zh. Eksp. Teor. Fiz.* **33**, 549 (1957)]; Z. Maki, M. Nakagawa and S. Sakata, *Prog. Theor. Phys.* **28**, 870 (1962); B. Pontecorvo, *Sov. Phys.–JETP* **26**, 984 (1968) [*Zh. Eksp. Teor. Fiz.* **53**, 1717 (1967)]; V. N. Gribov and B. Pontecorvo, *Phys. Lett. B* **28**, 493 (1969).
- [13] Chooz Collaboration, M. Apollonio *et al.*, *Phys. Lett. B* **466**, 415 (1999); M. Apollonio *et al.*, *Eur. Phys. J. C* **27**, 331 (2003) [hep-ex/0301017].

- [14] K. Anderson *et al.*, White paper report on using nuclear reactors to search for a value of  $\theta_{13}$ , hep-ex/0402041; F. Ardellier *et al.*, Letter of intent for Double-Chooz, hep-ex/0405032.
- [15] Y. Itow *et al.*, The JHF-Kamioka neutrino project, hep-ex/0106019; T. Kobayashi, Nucl. Phys. Proc. Suppl. **143** (2005) 303.
- [16] D. S. Ayres *et al.* [NOvA Coll.], hep-ex/0503053.
- [17] P. Huber, M. Lindner, T. Schwetz and W. Winter, Nucl. Phys. B **665** (2003) 487 [hep-ph/0303232]; P. Huber, M. Lindner, M. Rolinec, T. Schwetz and W. Winter, Phys. Rev. D **70** (2004) 073014 [hep-ph/0403068].
- [18] M. G. Albrow *et al.*, Physics at a Fermilab proton driver, hep-ex/0509019.
- [19] B. Autin *et al.*, Conceptual design of the SPL, a high-power superconducting H- linac at CERN, CERN-2000-012.
- [20] M. V. Diwan *et al.*, Phys. Rev. D **68** (2003) 012002 [hep-ph/0303081].
- [21] P. Zucchelli, Phys. Lett. B **532** (2002) 166.
- [22] C. Albright *et al.* [Neutrino Factory/Muon Collider Coll.], physics/0411123.
- [23] A. Blondel *et al.*, ECFA/CERN studies of a European neutrino factory complex, CERN-2004-002
- [24] J. E. Campagne and A. Cazes, Eur. Phys. J. C **45** (2006) 643 [hep-ex/0411062].
- [25] M. Mezzetto, J. Phys. G **29** (2003) 1771 [hep-ex/0302007]; J. Bouchez, M. Lindroos, M. Mezzetto, AIP Conf. Proc. **721** (2004) 37 [hep-ex/0310059].
- [26] A. de Bellefon *et al.*, MEMPHYS: A large scale water Čerenkov detector at Fréjus, Contribution to the CERN strategic committee,  
[http://apc-p7.org/APC\\_CS/Experiences/MEMPHYS/](http://apc-p7.org/APC_CS/Experiences/MEMPHYS/)
- [27] C. K. Jung, Feasibility of a next generation underground water Cherenkov detector: UNO, hep-ex/0005046.
- [28] K. Nakamura, Int. J. Mod. Phys. A **18** (2003) 4053.
- [29] P. Huber, M. Maltoni, T. Schwetz, Phys. Rev. D **71** (2005) 053006 [hep-ph/0501037].
- [30] P. Huber, M. Lindner and W. Winter, Comput. Phys. Commun. **167** (2005) 195 [hep-ph/0407333], <http://www.ph.tum.de/~globes>
- [31] P. Huber, M. Lindner and W. Winter, Nucl. Phys. B **645** (2002) 3 [hep-ph/0204352].
- [32] P. Lipari, M. Lusignoli and F. Sartogo, Phys. Rev. Lett. **74**, 4384 (1995) [hep-ph/9411341].
- [33] Webpage of the International Scoping Study physics working group:  
<http://www.hep.ph.ic.ac.uk/iss/wg1-phys-phen/index.html>

- [34] M. Mezzetto, Nucl. Phys. Proc. Suppl. **149** (2005) 179.
- [35] A. Donini, E. Fernandez-Martinez, P. Migliozi, S. Rigolin and L. Scotto Lavina, Nucl. Phys. B **710**, 402 (2005) [hep-ph/0406132].
- [36] J. Burguet-Castell, D. Casper, E. Couce, J. J. Gomez-Cadenas and P. Hernandez, Nucl. Phys. B **725** (2005) 306 [hep-ph/0503021].
- [37] P. Huber, M. Lindner, M. Rolinec and W. Winter, hep-ph/0506237.
- [38] J. Burguet-Castell, D. Casper, J. J. Gomez-Cadenas, P. Hernandez and F. Sanchez, Nucl. Phys. B **695** (2004) 217 [hep-ph/0312068].
- [39] F. Terranova, A. Marotta, P. Migliozi and M. Spinetti, Eur. Phys. J. C **38**, 69 (2004) [hep-ph/0405081].
- [40] M. Mezzetto, Nucl. Phys. Proc. Suppl. **143** (2005) 309 [hep-ex/0410083].
- [41] C. Volpe, J. Phys. G **30** (2004) L1 [hep-ph/0303222].
- [42] B. Autin *et al.*, J. Phys. G **29**, 1785 (2003) [physics/0306106]; M. Benedikt, S. Hancock and M. Lindroos, Proceedings of EPAC, 2004, <http://accelconf.web.cern.ch/AccelConf/e04>; M. Lindroos, EURISOL DS/TASK12/TN-05-02.
- [43] D. Casper, Nucl. Phys. Proc. Suppl. **112** (2002) 161 [hep-ph/0208030].
- [44] The NEUGEN neutrino event generator, <http://minos.phy.tufts.edu/gallag/neugen/>.
- [45] M. Mezzetto, hep-ex/0511005.
- [46] A. Fasso *et al.*, Proceedings of the MonteCarlo 2000 conference, Lisbon, October 26 2000, A. Kling *et al.* (eds.), Springer-Verlag Berlin (2001), 159-164 and 955-960.
- [47] Application Software group, Computing and Network Division *et al.*, GEANT Description and Simulation Tool, CERN Geneva, Switzerland
- [48] C. Catanesi *et al.* [HARP Coll.], CERN-SPSC 2002/019; D. Drakoulakos *et al.* [Minerva Coll.], hep-ex/0405002.
- [49] M. Mezzetto, J. Phys. G **29**, 1781 (2003) [hep-ex/0302005].
- [50] J. Burguet-Castell, M. B. Gavela, J. J. Gomez-Cadenas, P. Hernandez and O. Mena, Nucl. Phys. B **608** (2001) 301 [hep-ph/0103258].
- [51] H. Minakata and H. Nunokawa, JHEP **0110**, 001 (2001) [hep-ph/0108085].
- [52] G. L. Fogli and E. Lisi, Phys. Rev. D **54**, 3667 (1996) [hep-ph/9604415].
- [53] V. Barger, D. Marfatia and K. Whisnant, Phys. Rev. D **65**, 073023 (2002) [hep-ph/0112119].
- [54] O. Yasuda, New J. Phys. **6**, 83 (2004) [hep-ph/0405005].

- [55] M. Ishitsuka, T. Kajita, H. Minakata and H. Nunokawa, Phys. Rev. D **72** (2005) 033003 [hep-ph/0504026].
- [56] S. Antusch, P. Huber, J. Kersten, T. Schwetz and W. Winter, Phys. Rev. D **70**, 097302 (2004) [hep-ph/0404268].
- [57] H. Minakata, M. Sonoyama and H. Sugiyama, Phys. Rev. D **70** (2004) 113012 [hep-ph/0406073].
- [58] A. Donini, E. Fernandez-Martinez, D. Meloni and S. Rigolin, hep-ph/0512038.
- [59] O.L.G. Peres, A.Y. Smirnov, Nucl. Phys. B **680** (2004) 479 [hep-ph/0309312].
- [60] M.C. Gonzalez-Garcia, M. Maltoni, A.Y. Smirnov, Phys. Rev. D **70** (2004) 093005 [hep-ph/0408170].
- [61] S. T. Petcov, Phys. Lett. B **434** (1998) 321 [hep-ph/9805262]; M. Chizhov, M. Maris and S. T. Petcov, hep-ph/9810501; M. V. Chizhov and S. T. Petcov, Phys. Rev. Lett. **83** (1999) 1096 [hep-ph/9903399].
- [62] E. K. Akhmedov, Nucl. Phys. B **538**, 25 (1999) [hep-ph/9805272]; E. K. Akhmedov, A. Dighe, P. Lipari and A. Y. Smirnov, Nucl. Phys. B **542**, 3 (1999) [hep-ph/9808270].
- [63] J. Bernabeu, S. Palomares-Ruiz and S. T. Petcov, Nucl. Phys. B **669**, 255 (2003) [hep-ph/0305152].
- [64] C. W. Kim and U. W. Lee, Phys. Lett. B **444**, 204 (1998) [hep-ph/9809491].
- [65] T. Kajita, Talk at NNN05, 7–9 April 2005, Aussois, Savoie, France, <http://nnn05.in2p3.fr/>
- [66] M. C. Gonzalez-Garcia and M. Maltoni, Phys. Rev. D **70** (2004) 033010 [hep-ph/0404085].
- [67] S. T. Petcov and T. Schwetz, Nucl. Phys. B **740**, 1 (2006) [hep-ph/0511277].
- [68] O. Mena-Requejo, S. Palomares-Ruiz and S. Pascoli, Phys. Rev. D **72** (2005) 053002 [hep-ph/0504015]; hep-ph/0510182.
- [69] M. Kachelriess and R. Tomas, hep-ph/0412100.